

Depositional Facies and Detrital Composition of the  
Paleoproterozoic Et-Then Group, NWT, Canada:

Signature of  
Intracratonic Indentation Tectonics

by

Bradley D. Ritts  
B.S., University of Rochester  
(1993)

Submitted to the Department of  
Earth, Atmospheric and Planetary Sciences  
in Partial Fulfillment of the Requirements for the  
Degree of

MASTER OF SCIENCE  
in Geology

at the  
Massachusetts Institute of Technology  
May 1994

© 1994 Massachusetts Institute of Technology  
All rights reserved

Signature of Author .....  
Department of Earth, Atmospheric and Planetary Sciences  
March 1, 1994

Certified by .....  
John P. Grotzinger  
Thesis Supervisor

Accepted by .....  
Thomas H. Jordan  
Department Head

MASSACHUSETTS INSTITUTE OF TECHNOLOGY  
**WITHDRAWN**  
MAR 17 1994  
**MIT LIBRARIES**  
Linderoen

DEPOSITIONAL FACIES AND DETRITAL COMPOSITION OF THE  
PALEOPROTEROZOIC ET-THEN GROUP,  
NWT, CANADA: SIGNATURE OF INTRACRATONIC  
INDENTATION TECTONICS

by

BRADLEY D. RITTS

Submitted to the Department of Earth, Atmospheric, and Planetary Sciences  
on March 7, 1994 in partial fulfillment of the requirements for the Degree of  
Master of Science in Geology

ABSTRACT

Paleoproterozoic intracratonic compression across the Slave province resulted in eastward indentation of the wedge-shaped Slave craton into the Thelon orogen. Indentation was accommodated by shortening and crustal thickening at the apex of the Slave wedge, bounded to the south by the right-lateral McDonald fault and to the north by the left-lateral Bathurst fault. The Paleoproterozoic, non-marine Et-Then Group in the East Arm of Great Slave Lake records the history of this indentation.

The Et-Then Group consists of two formations. The older Murky Formation is an alluvial fan conglomerate deposited unconformably over older Paleoproterozoic sedimentary and igneous rocks and Archean metamorphic and igneous rocks. Clast composition indicates that the Murky Formation was derived from these older rocks, eroded during initial translation and uplift on the McDonald fault system. The Preble Formation conformably overlies the Murky Formation and is a braided fluvial sandstone. The modal framework composition of QFL 66, 28, 6; QmFLt 65, 28, 7 and P/F 0.37 indicates a granitoid source. On the basis of west-southwest paleocurrents, modal composition and depositional style the Preble Formation is interpreted to be derived from the Thelon orogen. Isostatic uplift at the apex of the Slave craton due to crustal thickening provided sufficient amounts of sediment to effectively bury local relief in the East Arm and change the depositional style from one of locally derived alluvial fans (Murky-style) to a westward-sloping, regionally extensive braid plain (Preble-style).

Thesis Supervisor: Dr. John Grotzinger

## ACKNOWLEDGEMENT

This work would not have been possible without the support of John P. Grotzinger, my advisor. John had the initial idea of looking for a project in the East Arm, and supported my first attempt at solo field work. Furthermore his thorough reviews of my work have improved this thesis.

Paul Hoffman has been invaluable in providing logistical assistance, ideas, and encouragement throughout this project. Discussions with him have greatly improved the quality of my work and often lead me in more interesting and productive directions, especially concerning regional geology.

Sunil Gandhi of the Geological Survey of Canada has provided industry data on the Et-Then Group, and has been more than willing to discuss other Paleoproterozoic non-marine basins of the northwestern Canadian shield. Sam Bowring has helped me to keep the geochronology straight, and provided perspective on regional issues.

Bill Padgham and the NWT Geology Division of Indian and Northern Affairs, Canada provided logistical support for the field work, as well as encouragement.

I appreciate the interactions that I have enjoyed with my fellow graduate students, particularly Shane Pelechaty who first identified the calcite grains in the Et-Then Group sandstones as possible soil pisoliths.

This work was completed in the first year of a National Science Foundation Graduate Research Fellowship to BDR. Support was also provided by National Science Foundation grant EAR-9058100 to Grotzinger.

Lastly, I want to thank Peter G. DeCelles and Gautam Mitra who introduced me to the worlds of sedimentology, sedimentary petrography, structural geology, and tectonics; and who continue to be an inspiration.

## TABLE OF CONTENTS

Title Page: 1

Abstract: 2

Acknowledgement: 3

Contents: 4

Text: 5

Introduction: 5

Regional Geology: 6

Previous Work: Et-Then Group: 8

Sedimentology: 9

Facies Trends: 13

Paleocurrent Directions: 14

Sedimentary Petrology: 15

Discussion: 22

Sedimentary Response to Indentation Tectonics: 23

Conclusions: 25

Figure Captions: 26

References: 28

Tables: 34

Figures: 40

## **Depositional Facies and Detrital Composition of the Paleoproterozoic Et-Then Group, NWT, Canada: Signature of Intracratonic Indentation Tectonics**

### **Introduction**

The analog model of plane indentation has been used extensively to explain the Cenozoic collision between India and Asia (Tapponnier and Molnar, 1976; Molnar and Tapponnier, 1975, 1977), and the present relationship between the Arabian plate and the Eurasian plate (McKenzie, 1972). The geometries of certain older orogenic belts also have been accounted for by indentation tectonics. A notable Proterozoic example is the Thelon orogen in the northwestern Canadian shield (Fig. 1).

Indentation tectonics first was proposed as an explanation for the Thelon orogen, the suture between the eastern Slave province and western Rae province, by Gibb (1978). Gibb noted the wedge shape of the Slave craton, the probable rheological difference between the older, more rigid Slave crust and younger, less rigid Rae crust, and the existence of large-scale structures matching the orientation and shear sense of slip lines in the indentation model (see figure 1 of Gibb, 1978). Hoffman (1980) first recognized the intracratonic nature of the indentation that was accommodated by the McDonald and Bathurst faults and linked the indentation to island arc accretion in Wopmay orogen. Hoffman (1987) advanced this analysis given the benefit of new information concerning the structure and kinematics of the Great Slave Lake shear zone, geochronologic constraints (Hanmer and Lucas 1985; Bowring et al, 1984), and regional paleomagnetic information (Geological Survey of Canada, 1987).

Hoffman (1988b, 1989) proposed a two-phase indentation model for the Slave-Rae collision. The first phase of indentation occurred along the Great Slave Lake shear zone during the attempted eastward subduction of the Slave craton beneath the Thelon orogen. The second phase of indentation was the result of post-collisional convergence between the Slave and Rae provinces along the younger Bathurst (north-northeast-striking, left-lateral) and McDonald (east-northeast-striking, right-lateral) transcurrent faults. This second indentation

corresponds temporally to the accretion of the Nahanni terrane in Wopmay orogen (Hoffman, 1988b) and occurred approximately 150 My following the initial Slave/Rae collision.

Henderson et al (1990) examined geophysical, isotopic and metamorphic evidence for the second, intracratonic indentation of the Slave craton into the Thelon orogen. They determined that between 1735 and 1840 Ma regional compression caused the Slave craton to indent farther into the Thelon orogen; indentation was accompanied by partial underthrusting of the eastern Slave craton beneath the Thelon orogen. This underthrusting and compression caused shortening and crustal thickening in the apical region (focus of the McDonald and Bathurst faults) of the Slave craton, as evidenced by the large paired gravity anomaly at the apex of the wedge. The thickening caused isostatic uplift in the eastern Slave province and Thelon orogen.

This paper addresses the sedimentary response to the second, ca. 1800 Ma, intracratonic indentation of the wedge-shaped Slave craton into the Thelon orogen along the Bathurst and McDonald fault systems. Siliciclastic sedimentary rocks of the syntectonic Et-Then Group record the tectonic development of the eastern and southern margins of the Slave craton during this phase of indentation. The Et-Then Group was deposited as the final phase of sedimentation in the Athapuscow basin, located in the East Arm of Great Slave Lake (Table 1). The sedimentology and provenance of the Et-Then Group provide additional geological constraints on the indentation event; this information may help to guide the interpretation of other tectonically similar sedimentary basins.

### **Regional Geology**

The northwestern Canadian shield (Fig. 1) is subdivided into two Archean provinces, formerly isolated micro-continents, and two Paleoproterozoic orogenic belts. The northwestern-most province in the Canadian shield is the Slave province. The Rae province lies to the south and east of the Slave province, separated by the Thelon-Taltson orogenic belt. Wopmay orogen flanks the western margin, and extends south and west of the Slave province.

The Slave province consists of greenschist to amphibolite facies 2660-2722 Ma metavolcanic, and 2.66-2.7 and 2.61 Ga metaturbidite complexes, associated with 2.58-2.7 Ga gabbroic to granitic plutonic rocks. 2.81-4.0 Ga granitoids, orthogneisses and metasedimentary rocks unconformably underlie the metavolcanics and metaturbidites in the western Slave craton (Bowring et al, 1990; Isachsen and Bowring, in review). The Slave province is bounded to the west by Wopmay Orogen, which includes several terranes accreted to the western margin of the Slave craton between 1.9 and 1.7 Ga (Hoffman, 1988b, 1989). The eastern and southeastern margins of the Slave abut rocks of the 2.0-1.9 Ga Thelon-Taltson orogen. On the southeastern edge of the Slave, the adjacent Thelon-Taltson rocks are deformed within the ca. 1900 Ma Great Slave Lake shear zone (Hoffman, 1987; Hanmer, 1988). The Great Slave Lake shear zone is a 25 km wide, right-lateral mylonite zone along which the Slave indented into the Thelon-Taltson magmatic arc during the ca. 1.9 Ga Slave/Rae collision (Grotzinger and McCormick, 1987; Hoffman, 1987, 1988b, 1989; Tirrul and Grotzinger, 1990).

The Rae province lies east of the Thelon orogen, and south of the Great Slave Lake shear zone. The Rae province consists of 2.6-3.1 Ga gneisses and meta-volcanics (Hoffman, 1989). The Rae is extensively deformed by Paleoproterozoic transcurrent faults, such as the Amer Lake shear zone and Ellis fault; some, including the Norman, MacInnis and King faults, formed non-marine pull-apart basins such as the Nonacho basin (Aspler and Donaldson, 1985).

The Bathurst and McDonald transcurrent faults form the northeastern and southeastern boundaries of the ca. 1800 Ma Slave wedge, respectively. The Bathurst fault system can be traced for about 350 km along a trend of 150° (Thomas et al, 1976). The most reliable estimate of the magnitude of left-lateral separation is 115 km, based on the projection of stratigraphic truncations across the Bathurst fault (Tirrul and Grotzinger, 1990). The McDonald fault system is traced for 550 km along its 060° trend (west of Great Slave Lake the interpretation of the fault is based on high-level aeromagnetic anomalies (Haines et al, 1971). Aeromagnetic anomalies suggest alternate interpretations of 125 km or 70 km of right-lateral separation (Thomas et al, 1976). Offset of geologic features in the East Arm suggest a right lateral

separation of about 70 km (Hoffman et al, 1977; Hoffman, 1988a), agreeing with the lesser estimate of Thomas et al (1976).

The Slave and Rae provinces contain several remnants of Paleoproterozoic sedimentary basins. The Kilohigok basin (Grotzinger and McCormick, 1987) is a remnant of a regionally extensive foreland basin formed during initial collision and underthrusting of the Slave craton in the Thelon orogen. The Et-Then Group, Athapuscow basin, in the East Arm of the Great Slave Lake (Hoffman, 1969, 1981; Hoffman et al, 1977; Ritts, 1994) and the Tinny Cove Formation of the Elu basin in Bathurst Inlet (Campbell, 1979) were deposited during the ca. 1800 Ma intracratonic indentation of the Slave into the Thelon. The Tinny Cove Formation is poorly exposed and not well studied. In contrast, the Et-Then Group is well exposed in the East Arm of the Great Slave Lake (Fig. 2) and has been the subject of study by Hoffman (1969) and Ritts (1994; this study).

#### **Previous Work: Et-Then Group**

The Et-Then Group is a sequence of non-marine, siliciclastic sedimentary rocks and minor basaltic volcanics and is formally divided into two formations (Stockwell, 1936). The older Murky Formation is 200 to > 1000 m of alluvial fan conglomerate (Hoffman, 1969). The Murky Formation grades into the overlying Preble Formation through a transition of approximately 20 m of interbedded pebble to cobble conglomerate and sandstone. The Preble Formation consists of fluvial sandstones and has a maximum thickness of at least 3000 m (Hoffman, 1969, 1988a). The volcanics occur primarily on the southern shore of Preble Island, intercalated with Murky Formation conglomerates. They are subaerial basalt flows of the continental tholeiitic type (unpublished data from S.E.R.U. Nucléaire (Canada) Limitée, cited by Gandhi and Loveridge, 1982).

Et-Then Group deposition is demonstrably contemporaneous with deformation on the McDonald fault zone. Murky and Preble Formation sediments are cut extensively by strands of



the McDonald fault system, and also depositionally overstep strands of the fault system (Fig. 3) (Hoffman, 1988a).

Previous work on the Athapuscow basin by Hoffman (1969) was the first to indicate that the Et-Then Group was deposited in response to deformation on the McDonald fault. Hoffman (1969) recognized the local provenance for much of the detritus in the Murky Formation, paleocurrent trends for the Preble Formation, proximal to distal and thickness relations in the Murky Formation, and correctly interpreted the alluvial depositional system. This data was cast into the geosynclinal model as a Taphrogeosyncline (normal fault bounded basins, deposited on older, deformed rocks; e.g. the Triassic Newark basin of the Appalachian orogen – Hoffman, 1969). Since then, developments in the regional geology of the Slave province and bounding Paleoproterozoic orogenic belts, the structural geology of the McDonald fault system (e.g.: Thomas et al, 1976; Gibb and Thomas, 1977; Hoffman et al, 1977; Gibb, 1978; Hoffman, 1987, 1988a, 1988b, 1989; Henderson et al, 1990; Tirrul and Grotzinger, 1990; Hanmer et al, 1992), and the sedimentology, stratigraphy and provenance of the Et-Then Group (Ritts, 1994; this study) have required the data to be recast into a new tectonic model.

### **Sedimentology**

The sedimentology and lithofacies of the Et-Then Group are briefly described here. More detailed descriptions are provided by Ritts (1994), including 950 m of measured sections. Locations of measured sections and other observation stations are shown in figure 4. Facies codes generally follow Miall (1978), and are explicitly defined by Ritts (1994).

#### **Murky Formation**

*Description:* The Murky Formation is composed of five lithofacies assemblages: Gmm, St/Sh, Sm/Sh/Sl, Gcm and carbonate/siltstone/Sr. The Gmm lithofacies assemblage (LA) is dominant. It consists of one to five meter-thick beds of red or buff colored, poorly bedded, massive, very poorly sorted, matrix-supported, cobble to boulder conglomerate (Fig. 5). Maximum clast sizes

are typically 30 to 50 cm in diameter, ranging to well over one meter. A few thin, silty mud layers, some with distinct to partly coalesced limestone nodules and/or desiccation cracks also are present. Bedding is lenticular to tabular on outcrop scale (Fig. 7a).

The remaining LAs make up only a minor amount of the Murky Formation. The St/Sh LA consists of 0.3 to 2.5 m thick beds of buff-colored, medium to well sorted, medium to granular, trough cross-stratified and plane-bedded sandstones. Beds have erosional bases and often pinch and swell, with an overall lenticular to tabular geometry on outcrop scale (Fig. 5). Some beds show distinct fining or coarsening-upward sequences (Fig. 7b). The Sm/Sh/SI LA consists of buff-colored, decimeter-scale beds of medium to very coarse, medium sorted, plane-bedded and low-angle cross-bedded sandstone with sharp bases. Also present are meter-scale beds of massive, very coarse, very poorly sorted sandstone with floating pebbles and non-erosional bases. Primary current lineations and small-scale ripple marks often occur in the plane bedded and low-angle cross-bedded lithofacies. Uncommon desiccation cracks and limestone nodules are found in finer grained interbeds associated with the two sandstone LAs. The Gcm LA consists of 0.5 to 3 m thick beds of poorly bedded, massive, poorly sorted, very angular, monolithologic, pebble to boulder, clast-supported breccia (Fig. 5).

The carbonate/siltstone/Sr lithofacies (carbonate LA of Ritts, 1994) consists of 0.5 to 2 m thick beds of stromatolitic limestone or dolomite and bulbous 2 m high stromatolite heads surrounded by red siltstone matrix (Hoffman, 1969, 1976). Most are fine grained and recrystallized. The carbonate beds are often associated with rippled, massive and laminated, red silts and clays, some with desiccation cracks, up to 10 meters thick (Hoffman, 1969, 1976). The Sr lithofacies is red, medium grained, well sorted sandstone with small-scale, two-dimensional, symmetric and asymmetric ripple marks and horizontal lamination, often with desiccation cracks.

*Interpretation:* The silty beds with limestone nodules are interpreted as calcretes (Theriault and Desrochers, 1993). The interpretation of the limestone nodules as an early pedogenic feature is supported by the presence of intrabasinal soil pisoliths as detrital grains in

interbedded sandstones (discussed below). Hoffman (1969) also interpreted some of the calcareous horizons in the Murky Formation as paleosols. The desiccation cracks and paleosols found in the Murky Formation are interpreted to indicate subaerial exposure. The mechanisms for deposition of the Gmm, St/Sh and Sm/Sh/SI LAs are interpreted to be debris flow, channelized, sub-aqueous traction (stream flow), and a combination of mud flow (Sm) and sheetflood (Sh and SI), respectively (Hooke, 1967; Bull, 1968; Hooke and Rhorer, 1979). These LAs are interpreted to represent an alluvial fan depositional system. The debris flows are characteristic of inner and mid-alluvial fan environments and the mud flows and sheetfloods would be typical of a mid to outer alluvial fan (Hooke, 1967; Bull, 1968; Hooke and Rhorer, 1979). The streamflow deposits of the St/Sh LA are typical of an entrenched fan or distributary channels on an outer fan (Hooke, 1967; Bull, 1968; Hooke and Rhorer, 1979). The Gcm LA is interpreted to be a talus breccia, based on its monolithologic, very angular, clast supported nature and because it is found only adjacent to fault strands. The limestones, dolomites, and silty mudstones of the carbonate/siltstone/Sr LA are interpreted to be lacustrine sediments (Hoffman, 1976) based on the presence of stromatolites, laminated sediments (generally low energy conditions) and association with alluvial fan and fluvial strata. The rippled and laminated sandstones of the carbonate/siltstone/Sr LA are interpreted to be shallow water and shoreline lacustrine equivalents of the carbonates and siltstones (Picard and High, 1981).

### Preble Formation

*Description:* The Preble Formation has a dominant St/Sh/SI LA and a minor Gmm/Sh/SI/Sm LA. The St/Sh/SI LA consists of medium to very well sorted, fine to very coarse, red and buff mottled sandstone (Fig. 5). Primary sedimentary structures include trough cross-stratification, primary current lineation, planar lamination, and uncommon small-scale, two-dimensional ripple marks (mostly asymmetrical, few symmetrical and interference) and ripple cross-lamination. In the lower 300 - 400 m of the formation grain size is coarser and 0.4-2.5 m thick,

coarsening-up beds are common. In stratigraphically higher parts of the formation grain size fines slightly, bed thicknesses remain fairly consistent and fining-upward beds become more common. Beds have sharp or scoured bases, often with mud chips or a gravel lag at the base of the bed. Bedding on outcrop scale has lenticular geometry. A few interbedded millimeter to centimeter-scale red and green mud layers, some with desiccation cracks (Fig. 6), occasionally overlie rippled or planar-laminated beds (Figs. 5, 7d).

The Gmm/Sh/SI/Sm LA consists of the Gmm/Sm and Sh/SI sub-LAs. The Gmm/Sm sub-LA consists of 1.5 to 2 m thick beds of poorly sorted, massive, matrix-supported, pebble to cobble conglomerate and 0.5 to 1.5 m thick beds of very poorly sorted, coarse to granular, massive, red-buff sandstone with floating pebble and cobble clasts. Beds are roughly tabular on outcrop scale with sharp bases. The Sh/SI sub-LA consists of centimeter to decimeter-scale beds of medium to well sorted, fine to medium grained, planar-laminated and low-angle cross-stratified sandstones with primary current lineations and asymmetric and (few) symmetric, two dimensional, small-scale, straight crested ripple marks. Bedding is tabular on outcrop scale with sharp bases (Fig. 7e).

Soft-sediment deformation, including convolute bedding, overturned cross-bedding (recumbent-folded of Allen and Banks, 1972), and load casts, is common in the Preble Formation, particularly the St/Sh/SI lithofacies. Liesegang banding is also characteristic of the Preble Formation.

*Interpretation:* The St/Sh/SI LA is interpreted as channelized, sub-aqueous, traction deposits formed within a sandy braided fluvial system (Miall, 1978; Rust, 1978). Interbedded mudstones with desiccation cracks indicate subaerial exposure and are interpreted as overbank deposits. The depositional process for the Gmm/Sm and Sh/SI sub-LAs was debris and mud flow, and sheetflood, respectively. The depositional system of this LA is interpreted to be relatively small sediment lobes debauching into the fluvial system from minor rejuvenated relief on the

mostly buried McDonald fault system. Many of the rippled sandstones occur as waning-stage flood deposits in overbank areas and on bars. However, on the two islands 8 km northeast of Snowdrift and on the large island south of Basile Bay (and east of Union Island) meter-scale sections of thin, planar beds of fine-medium sandstone with asymmetric, symmetric, and interference ripple marks, planar lamination and desiccation cracks are interpreted to be shallow water and shoreline lacustrine deposits (Picard and High, 1981).

The soft-sediment deformation features in the Preble Formation fit the description of deformation features caused by liquefaction during seismic activity (Keunen, 1958; Allen and Banks, 1972; Sims, 1973, 1975; Hempton and Dewey, 1983). The types of deformation features, close association with the McDonald fault zone, and restriction of deformed zones to discrete stratigraphic horizons, sometimes involving more than one bed, suggest the role of seismicity in producing the soft-sediment deformation (Sims, 1973, 1975).

### **Facies Trends**

Murky Formation facies become more proximal to the southeast, nearer to the McDonald fault system. The most proximal facies are talus breccias and thick, poorly-bedded debris flow deposits. These facies grade northwestward into more distal fan facies with significant fluvial sequences and minor lacustrine rocks (Ritts, 1994). Furthermore, maximum clast sizes decrease from southeast to northwest (Hoffman, 1969). Along the length of the East Arm these relationships remain consistent within the Murky Formation. In the Preble Island area, the Murky Formation consists entirely of proximal debris flow conglomerates. These trends are consistent with the interpretation of the Murky Formation as a transverse filling alluvial fan or bajada system draining from the McDonald fault system.

The Preble Formation records a sandy, braided fluvial system along the length of the East Arm, generally showing no discernible along-strike facies changes. This observation is consistent with the interpretation of the Preble Formation as a longitudinal fluvial system draining from a distal source. In the southeastern part of the basin, very close to strands of the

McDonald fault system, the sheetflood sandstones, mud-flow sandstones and debris flow pebble conglomerates, interpreted as transverse sediment lobes, occur as minor components relative to the fluvial facies.

### **Paleocurrent Directions**

Paleocurrent data were collected from trough cross-stratification, primary current lineations, small-scale ripple marks, and imbricated, clast-supported, pebble-cobble conglomerates. Between 10 and 50 indicators from any given bed were measured, then averaged to give a paleocurrent direction for that bed. Trough cross-stratification yields paleocurrent data from the direct measurement of trough axes, as well as the measurement of limb sets. Paleocurrent directions are derived from trough limbs by measuring the orientations of ten left and ten right limbs per cross-bed set. These limb attitudes yield a paleocurrent direction, using method I of DeCelles et al (1983). Correction for tectonic dip was made on all raw data.

Paleocurrent directions in the Murky Formation are interpreted from trough axes and limbs, and imbricated, clast-supported, pebble-cobble conglomerates. Throughout the basin, Murky Formation paleocurrents are dominantly to the northwest. Most are between  $282^{\circ}$  and  $001^{\circ}$ , with a mean vector of  $332^{\circ}$  (see figure 8a). All of the paleocurrent indicators show flow in a radial pattern to the northwestern side of a line trending  $052^{\circ}$ . These data are consistent with an alluvial fan depositional system draining from a  $060^{\circ}$ -trending paleohigh on the McDonald fault.

Paleocurrent directions in the Preble Formation are interpreted from trough axes and limbs, and primary current lineations. The mean paleocurrent vector for the Preble Formation is  $266^{\circ}$  (see figure 8b). Hoffman (1969) derived a mean paleocurrent direction of  $257^{\circ}$  from over 1000 paleocurrent indicators. This west-southwest paleocurrent is consistent with an axial fluvial system parallel to the trace of the McDonald fault.

The northward-directed component of Preble Formation paleocurrents were measured primarily from traction deposits in the LA interpreted as sediment lobes debauching into the

fluvial system from the McDonald fault system. These paleocurrents confirm a minor transverse input of sediment from the McDonald fault zone during Preble deposition.

### **Sedimentary Petrology**

The petrology and provenance of the Et-Then Group was determined with conglomerate clast counts in the Murky Formation and sandstone point counts in the Murky and Preble Formations.

#### **Conglomerate Petrology**

##### **Methods**

Counts were made of at least 100 pebble to boulder-size clasts per bed. Clast counts were made in the Murky Formation at Murky Channel, Et-Then Island, Preble Island, and the islands 8 km northwest of Snowdrift. Clast types, briefly described below, were defined at the outset of the study. However, any distinguishing characteristics such as heavy mineral bands in quartzite clasts also were noted. A special effort was made to match clasts to their sources in the Great Slave Supergroup, Wilson Island Group and Great Slave Lake shear zone.

##### **Clast Types**

*Quartzite:* Variably cemented or recrystallized quartzose sandstones. Many are micaceous or have heavy mineral bands and/or cross-bedding. Most are derived from the Sosan Group, particularly the Kluziai and Hornby Channel formations, but also from the Wilson Island Group.

*Shale:* Red, green, dark gray shale, mudstone or fine siltstone. Some of the gray shales are graphitic, while others have cleavage. Red and green shales primarily are derived from the Kahochella Group; gray shales mostly are from the Wilson Island Group. No clasts of typical Union Island Group black, graphitic shale were observed.

*Carbonate:* Grey, tan or reddish limestones or dolomites, often with chert stringers and microbial? lamination. These probably are derived from the Duhamel Formation of the Sosan Group.

*Granitoid:* Undeformed, orange granitoids, typical of the Slave lithologies found in the basement to Athapuscow basin sedimentary rocks, and mylonites, characteristic of the Great Slave Lake shear zone. In most cases mylonite clasts can be matched with specific source belts in the Great Slave Lake shear zone (Hanmer, 1988).

### **Conglomerate Compositional Trends**

Histograms showing the conglomerate clast lithology of the six measured sections are shown in figure 9, from data in table 2. East of 112° the Murky Formation has a lower shale-clast "member" (0 to 450 meters thick), replaced by a quartzite-clast "member" (250 to 450 meters thick). At Murky Channel, proximal to the McDonald fault system, the shale-clast conglomerate accounts for about the lower fifty percent of the formation. The shale-clast conglomerate thins away from the McDonald fault system and pinches out before Et-Then Island. West of 112° over 90% of the Murky Formation consists of granitoid and mylonite-clast conglomerates. The remainder of the formation consists of randomly intercalated 20-40 m thick carbonate-clast conglomerates. In sections on the south shore of Preble Island, associated with the volcanics, carbonate-clast conglomerates are missing.

The disparity in Murky Formation petrofacies between east of 112° and west of 112° is the result of a complex source terrane. The lack of a uniform composition in the Preble Island area, in contrast to the consistent composition east of 112°, is the result of deposition being quasi-partitioned into small basins controlled by splays of the McDonald fault system (Hoffman, 1969). This partitioning is manifested in the abrupt changes from sections with carbonate clasts to those without carbonate clasts, and thickness variations over fault strands.



## **Provenance**

Clasts in the Murky Formation east of 112° are all derived from the Great Slave Supergroup (Sosan and Kahochella Groups) and the Wilson Island Group. The shale clasts in the shale-clast conglomerate are derived from the Kahochella and Wilson Island groups. The quartzite clasts in the quartzite-clast conglomerate are derived almost entirely from the Kluziai and Hornby Channel Formations of the Sosan Group. The Wilson Island Group also was a minor source for the quartzite-clast conglomerate.

In the Preble Island area, Murky Formation clasts are derived mostly from the Great Slave Lake shear zone and Archean crystalline rocks of Slave basement with minor, but locally significant input from the Great Slave Supergroup (Sosan Group). Undeformed granitoid clasts are derived from Archean Slave basement and Paleoproterozoic Thelon-Taltson protoliths of the Great Slave Lake shear zone. The present-day erosion level exposes abundant Archean granite in the Preble Island area (Slave), as well as the Taltson granitoids unaffected by the Great Slave Lake shear zone. Similar lithologies were exposed to erosion during deposition of the Murky Formation. The mylonitic and foliated granitoid clasts are derived from the Great Slave Lake shear zone. Clasts derived from each belt of the shear zone (Hanmer, 1988) can be identified. The carbonate clasts are derived from the Duhamel Formation of the Sosan Group. All of these sources are local to the East Arm.

The mix of clast lithologies, with no apparent systematic variation related to unroofing, is accounted for by the complexity of the eroding source terrane. The East Arm had experienced at least one phase of fold and thrust deformation and one phase of transpressional deformation prior to McDonald fault-related transcurrent faulting (Table 1). These deformations resulted in a complex exposure pattern in the East Arm.

## Sandstone Petrology

### **Methods**

Sandstone samples were collected from measured sections in the vicinity of Preble Island, Et-Then Island, Redcliff Island, Murky Channel, Basile Bay, Union Island and the two islands 8 km northwest of Snowdrift (Fig. 4). Samples were cut into thin sections and half of each was stained for plagioclase and potassium-feldspar. 105 stained thin sections were point counted (450 grains/slide) on a flat-stage petrographic microscope with an automatic point-counter using the Gazzi-Dickinson point-counting method (Dickinson, 1970; Ingersoll et al, 1984). Grain parameters are briefly described below (Table 3). The raw data (Table 4) were then recalculated into QFL%Q, QFL%F, QFL%L, QmFLt%Qm, QmFLt%F, QmFLt%Lt and P/F for each sample, as well as mean values and standard deviations for the data and various subsets of samples (see table 4).

### **Grain Types**

*Monocrystalline Quartz:* Monocrystalline quartz (quartz crystal  $\geq 0.0625$  mm in diameter) totals about 56% of the grains counted. A few grains, restricted to the Murky Formation, show secondary quartz overgrowths (Fig. 10). About 83% of the monocrystalline quartz grains show undulose extinction.

*Potassium Feldspar:* K-feldspar (K-feldspar crystal  $\geq 0.0625$  mm in diameter) makes up about 16% of the grains counted (Fig. 10). Many grains show partial alteration to phyllosilicates and/or corroded boundaries replaced by quartz.

*Plagioclase:* Plagioclase (plagioclase crystal  $\geq 0.0625$  mm in diameter) makes up about 9% of the grains counted (Fig. 10). Plagioclase is often partially altered to phyllosilicates.

*Sedimentary Lithics:* Fine grained shale, siltstone and mudstone fragments make up about 3% of the grains counted. Most are aggregates of phyllosilicates, sub-sand-sized quartz and iron oxides.

*Volcanic Lithics:* Fine grained quartz or feldspar groundmass with plagioclase or phyllosilicate micro-laths made up approximately 1% of the grains counted.

*Other Lithics:* Fine grained lithic fragments that could not be confidently placed into Ls, Lv or Lm make up 2% of the grains counted. These were typically aggregates of microcrystalline quartz, phyllosilicates and/or sub-sand-sized quartz and/or plagioclase that could not be distinguished as Lv or Ls or vaguely foliated varieties that could not be distinguished as Lm or Ls.

*Others:* Grains that were counted, but made up less than 1% of the modal framework were (in decreasing abundance): polycrystalline quartz (quartz aggregate with counted sub-grain < 0.0625 mm in diameter), metamorphic lithics, chert and phyllosilicates (phyllosilicate grain  $\geq$  0.0625 mm in diameter).

Other grains, not counted in the modal framework, include detrital accessories: amphibole, zircon, tourmaline; and intrabasinal, calcitic pisoliths (Fig. 10). The detrital accessories are those commonly found in sandstones. The pisoliths are 0.5-2 mm, concentrically layered, inclusion-rich calcite grains. The centers of the pisoliths are either dark mud, or calcite-cemented pellets of silt-size quartz grains. Many of the pisoliths are broken or penetrated by other detrital phases. These grains are interpreted as pedogenic calcrete pisoliths (similar to features described by Pelechaty and James, 1991, and Theriault and Desrochers, 1993) eroded from overbank areas and deposited in nearby channels, macroforms or sediment lobes.

The constituent minerals of coarse-grained rock fragments were counted, in accordance with the Gazzi-Dickinson point-counting method (Dickinson, 1970; Ingersoll et al, 1984). Sandstone grains are the most common coarse-grained rock fragments in the Murky Formation (Fig. 10). These sandstone grains contain potassium feldspar and lesser plagioclase, but are dominantly monocrystalline quartz. Aggregates of two to four crystals of monocrystalline quartz, potassium feldspar and/or plagioclase are not uncommon, in the Preble Island area. The Preble Formation has rock fragments consisting of two to four crystals of monocrystalline quartz and potassium feldspar (rarely plagioclase). The coarse quartz/feldspar aggregates in the Preble Formation

and Murky Formation (near Preble Island) are granitoid rock fragments. Quartzose mylonite rock fragments are very common accessories in the Preble Formation, and in the Murky Formation near Preble Island (Fig. 10), but are counted as Qm or Qp depending on sub-grain size.

The feldspars observed during this study were all identifiable by staining, twinning and/or alteration. Most altered feldspar grains were still clearly recognizable, based on a gradation from pristine feldspar crystals, to those that were almost completely altered to phyllosilicates. Even highly altered grains commonly retained ghost twinning and accepted the appropriate feldspar stain.

### **Modal Sandstone Composition**

Et-Then Group sandstones have a mean QFL of 66, 26, 8 and a mean QmFLt of 65, 26, 9. The Murky Formation sandstones have mean QFL 68, 20, 12 and mean QmFLt 67, 20, 13 (Fig. 11). Preble Formation sandstones have mean QFL 66, 28, 6 and mean QmFLt 65, 28, 7 (Fig. 11). Mean P/F ratio for the Preble Formation is 0.37. The mean P/F ratio for the Murky Formation is 0.24.

### **Compositional Trends**

Compositional trends of Murky Formation sandstones generally reflect those established for the conglomerates. Samples from east of 112°, interbedded with sedimentary clast conglomerates, show an enrichment in Q and L relative to F (Fig. 12a). This confirms the petrofacies defined by clast compositions in the Murky Formation conglomerates. Samples from the Preble Island area, interbedded with mylonite and granitoid clast conglomerates, show an enrichment in F relative to Q and L. In addition, they show an enrichment in plagioclase relative to K-feldspar, with a P/F ratio of  $0.57 \pm 0.09$ .

The Preble Formation has a uniform QFL and QmFLt composition throughout the East Arm. All of the localities lack systematic vertical variation in composition. Samples from the Preble Island area display a slight enrichment in F relative to samples from the Preble Formation east of 112°. The Preble Island area samples have mean QFL 56, 37, 7 and QmFLt 55,

37, 8 relative to mean QFL 65, 30, 5 and QmFLt 64, 30, 6 for the other localities (Fig. 12b). The P/F ratio of the Preble Formation shows no systematic vertical or lateral trends.

### **Provenance**

Murky Formation sandstone compositions plot in the "Recycled Orogen" field of the QFL diagram and straddle the "Transitional Basement", "Mixed" and "Recycled Orogen" fields of the QmFLt diagram of Dickinson et al (1983) (Fig. 11). These data agree with the conglomerate-based interpretation of a local East Arm provenance for the Murky Formation. The wide scatter and mix of provenance types, as with the conglomerates, is explained by the complexity of exposure in the East Arm source terrane. Sandstones found interbedded with the mylonite and granitoid clast conglomerates of the Preble Island area are also interpreted to be derived from the Great Slave Lake shear zone. These sandstones are enriched in F and have high P/F ratios.

Preble Formation sandstones plot in the "Transitional Basement" field on the QFL and QmFLt diagrams of Dickinson et al (1983) (Fig. 11). Given west-southwest-directed paleocurrents and more distal facies relative to the Murky Formation, Preble Formation sandstones are interpreted to be derived from the crystalline rocks uplifted at the apex of the Slave wedge, rather than from similar lithologies in the Great Slave Lake shear zone. Additional evidence suggesting derivation from the Slave apex for the Preble Formation is provided by contrasts in P/F ratio in the Et-Then Group. The P/F ratio of the Preble Formation is a uniform  $0.37 \pm 0.13$ . In contrast, the P/F ratio of Murky Formation sandstones interbedded with mylonite clast conglomerates, known to be derived from the Great Slave Lake shear zone is  $0.57 \pm 0.09$  (Fig. 13). This difference in P/F ratio may reflect differences in source rock mineralogy or preferential loss of plagioclase relative to potassium-feldspar over the longer transport distance from the apex of the Slave indentor. In either case the difference is significant and allows the distinction of Great Slave Lake shear zone-derived petrofacies from

Thelon orogen-derived petrofacies, supporting the hypothesis that the Preble Formation is derived from the apex of the Slave indentor.

The tendency for Preble Formation samples in the Preble Island area to be slightly enriched in F and for samples from east of 112° to be slightly enriched in Q (Fig. 12b) may be due to dilution of the apex-derived sediment with minor input from local sources. Minor input of local East Arm detritus into the Preble Formation is supported by the sedimentologic observations of transverse-filling sediment lobes, marked by the Gmm/Sh/SI/Sm LA, and a component of northward directed paleocurrents. This input would skew modal sandstone composition toward the Q pole east of 112° where local sources are sedimentary rocks of the Great Slave Supergroup and Wilson Island Group. The local input would shift modal composition toward the F pole in the Preble Island area where source rocks are dominantly Archean and Proterozoic granitoids.

East of 112°, mylonite grains occur only in the Preble Formation. They occur in both the Murky and Preble formations near Preble Island. This supports the conclusion that east of 112° the Murky Formation is derived from sedimentary cover while the Preble Formation is derived from mylonitized granitoids at the Slave apex. The mylonite grains in the Murky Formation are derived from the adjacent Great Slave Lake shear zone.

## Discussion

The sedimentology and petrology of the Et-Then Group (Fig. 14, table 5) records shifting areas of deformation and source area during the intracratonic indentation of the Slave province into the Thelon orogen. Compression across the Slave craton activated the McDonald and Bathurst transcurrent faults and displaced the Slave to the east, relative to the Rae province. In the East Arm this initial deformation produced relief on the southern side of the McDonald fault system due to a south-side-up component of dip-slip, creating a sediment source and accommodation space in the proximal Athapuscow basin. The McDonald fault system supplied coarse, local detritus from the Great Slave Supergroup, Wilson Island Group, and Great Slave Lake shear zone to northwest-prograding alluvial fans of the Murky Formation.

At the apex of the Slave wedge, indentation of the Slave craton into the Thelon orogen resulted in underthrusting of the Slave craton, crustal thickening, and isostatic uplift (Henderson et al, 1990). Uplifted rocks exposed an extensive source of granitic rocks to erosion. This detritus was supplied to the Athapuscow basin by west-southwest flowing braided rivers, restricted to the southeast by uplands south of the McDonald fault zone. The volume of sediment supplied in this manner was sufficient to bury most of the strike-slip relief in the East Arm and deposit a thick blanket of sand over the basin. Continued deformation on the McDonald and Bathurst fault systems sustained uplift and sediment supply from the Slave apex and locally rejuvenated uplift on the McDonald fault system, adding minor sediment sources within the East Arm.

#### **Sedimentary Response to Indentation Tectonics**

It should be emphasized that the Et-Then Group is an example of the sedimentary record of *intracratonic* indentation. That is, the two micro-continents (Slave and Rae) had sutured over 100 My in advance of this post-collisional convergence and reactivation of the suture (Henderson et al, 1990). The sedimentary record associated with a collisional indentation scenario (such as the initial Slave/Rae collision and indentation of Hoffman, 1987, 1988b, 1989) may be different from the one described below, because in the former case uplift would be maintained in the collisional orogen throughout the indentation, possibly obscuring early transform-related sedimentation.

It is difficult to develop a general model for sedimentation in response to intracratonic indentation. Depositional systems, sediment composition and vertical succession of facies, provenance and paleocurrents will vary greatly depending on tectonic influences, such as rates of uplift and subsidence, source rock lithology and location relative to the apex of the indenter, climatic influences and sea level. However, sedimentary signatures can be predicted for basins in some critical areas relative to the apex of the indenter (Fig. 15).

Perhaps the best place for interpreting a tectonic indentation from the sedimentary record is at the indenter margin, along the transcurrent structures that accommodate the indentation. This position, relative to the apex of the indenter, gives evidence for the early transcurrent faulting in the immediate vicinity of the basin, and also will eventually show detrital input from the apex of the indenter. The Et-Then Group in the Athapuscow basin occupies this position for the Slave/Rae indentation. There is one particularly important aspect of Et-Then sedimentation that may be applicable to other similar basins in the geologic record. This is the change from sediment derived locally from drainage systems transverse to transcurrent faults to exotic detritus delivered by a longitudinal drainage system tapping distal sources. In the former case, sedimentation is dominated by proximal depositional systems and deposited in relatively narrow, strike-slip basins (Christie-Blick and Biddle, 1985). This contrasts with the latter case, in which sedimentation is dominated by broad, relatively distal depositional systems that fill strike-slip basins in addition to forming a widespread blanket deposit.

Since the indentation model predicts the extrusion of crustal blocks by transcurrent faulting in the indented plate, one expects to see the development of trans-tensional pull-apart basins in the indented plate. However, an isolated pull-apart basin preserved in the ancient record is not necessarily the result of transcurrent faulting due to indentation.

Immediately to either side of the uplifted apex, one would expect to see a coarse clastic wedge prograding from the area of uplift. In the case of the Slave indenter, no sedimentary rocks are preserved directly adjacent to the inferred area of uplift on the Slave craton. The Thelon basin occupies this position on the Rae craton and may be of the same age (Loveridge et al, 1988). However, available data from Donaldson (1965) suggest that these units were derived from the east. In general, one would expect the record in these adjacent basins to show uplift and erosion, not unlike the record that might be found in a foreland basin.

Composition of the sediment will be governed by source rock lithology (which is in turn dependent on previous tectonic history and erosion levels) and climate. For this reason compositional data can not be used independently to identify transform and indentation



settings, as Dickenson and Suczek (1979) and Dickinson et al (1983) have successfully done for other types of basins (Ridgway and DeCelles, 1993).

## Conclusions

The final phase of deformation in the Thelon orogen was a ca. 1800 Ma indentation of the Slave microplate along the McDonald and Bathurst fault systems. In the Athapuscow basin, the Et-Then Group was deposited concurrently with motion on the McDonald fault and thus represents synorogenic sedimentation related to this post-collisional convergence. Et-Then Group lithofacies and petrofacies demonstrate the progression of tectonic indentation.

The first record of continental transcurrent deformation associated with the McDonald fault system are the proximal alluvial fan deposits of the Murky Formation, derived from the uplifted southern side of the McDonald fault system. Sedimentary evidence for continued deformation on the McDonald fault system occurs in the Preble Formation as possible seismites, and minor rejuvenated sediment lobes derived from the McDonald fault system to the southeast. For the most part, however, the Preble Formation is characterized by a sandy braided river depositional system that buried the Athapuscow basin and most of the McDonald fault system in northeasterly-derived, granitoid detritus indicating uplift in the Thelon orogen and eastern Slave craton at the apex of the Slave wedge.

In general, sedimentary rocks derived from uplifts caused by indentation may be widely variable in depositional systems and compositions, depending on rates of uplift, source rock lithologies, location relative to the apex of the indenter, sea level, and climate. However, basins located along transcurrent margins associated with indentation may be expected to show a change from local, transverse (relative to the transcurrent structures) sedimentation to more distal, longitudinal (relative to the transcurrent structures) sedimentation that overwhelms local relief and sediment supply.

## Figure Captions

**Figure 1:** Tectonic map of the northwestern Canadian shield, modified after Hoffman (1989) and McCormick and Grotzinger (1992).

**Figure 2:** Geologic map of Athapuscow basin. Dark lines indicate right-lateral transcurrent faults. Geology by Hoffman (1988a). PI, Preble Island; UI, Union Island; BB, Basile Bay; ET, Et-Then Island; MC, Murky Channel; RC, Redcliff Island; SD, Snowdrift. Box centered on MC indicates area of figure 3.

**Figure 3:** Detailed geologic map of the Murky Lake area. Dark lines are right-lateral transcurrent faults, dark lines with barbs are thrust faults, dark lines with balls are normal faults. Map shows unconformable relationship between the Et-Then Group and the older Great Slave Supergroup, Wilson Island Group, Compton laccoliths, and thrust faults. The Fortress gabbro intrudes all units, and cross-cuts the transcurrent faults. East of Basile Lake, the upper Murky Formation depositionally oversteps the first splay fault; the upper Preble Formation depositionally oversteps the second. Geology by Hoffman (1988a).

**Figure 4:** Location map for measured sections and other important localities.

**Figure 5:** Representative lithofacies of the Murky Formation (A, B, C, D) and Preble Formation (E, F). A) boulder Gmm near Preble Island; B) pebble to cobble Gcm breccia near Murky Channel; C) channelized debris flow Gmm on Et-Then Island; D) channelized sandstone of the St/Sh LA in debris flow Gmm on Et-Then Island; E) St/Sh/SI LA on Et-Then Island (arrow points to rock hammer for scale); F) rare mud interlayers on Et-Then Island.

**Figure 6:** Sandstone casts of desiccation cracks from the St/Sh/SI LA of the Preble Formation on the island south of Basile Bay and east of Union Island.

**Figure 7:** Representative measured sections through important Et-Then Group facies. A) proximal Murky Formation Gmm LA from Murky Channel; B) distal Murky Formation fluvial sequence at Et-Then Island; C) Murky Formation/Preble Formation transition south of Murky Channel; D) typical Preble Formation fluvial facies from of Basile Bay; E) Preble Formation Gmm/Sh/SI/Sm LA along the south side of Murky Channel. Arrows indicate paleocurrent

directions. Horizontal axis shows mud, fine, medium, and coarse sand, pebble, cobble and boulder grain size increments.

**Figure 8:** Et-Then Group paleocurrent directions. The perimeter of the circle equals 20%.

**Figure 9:** Stacked pie diagrams showing clast compositions for the Murky Formation. Outer circle is the lowest sample in the section (Table 2), inner circle is highest. Section locations: A) north side of Murky Channel; B) south shore of Et-Then Island; C) islands 8 km northwest of Snowdrift; D) islands off southwest corner of Preble Island.

**Figure 10:** Photomicrographs from Murky Formation (A, B, and E) and Preble Formation (C, D, F) sandstones. Scale bar (lower right) is 1 mm in each photograph. A) Qm grain from Murky Formation with secondary quartz overgrowth (arrow); B) sandstone rock fragment; C and D) mylonite grains; E) calcitic pisolith with silt-sized quartz grains in center; F) recrystallized calcite pisolith (center, large arrow), plagioclase crystal (center bottom, small arrow), and microcline crystal (center top, small arrow).

**Figure 11:** Framework sandstone compositions from the Et-Then Group. Crosses represent individual samples; polygons show standard deviation; means (not shown) plot at centers of polygons. Grid lines and provenance fields are from Dickinson et al (1983).

**Figure 12:** Mean and range of sandstone compositions west and east of 112°.

**Figure 13:** P/F ratio for Great Slave Lake shear zone-derived sandstones in the Murky Formation (Emg) versus P/F ratio for the Preble Formation sandstones (Ep).

**Figure 14:** Summary of Et-Then Group stratigraphy, facies, composition and paleocurrent directions. Arrows represent paleocurrent directions. Dark lines indicate dominant composition: s, shale; q, sandstone or quartzite; c, carbonate; and g, granitoid. Grain size axis and lithofacies are the same as for figure 4.

**Figure 15:** Map of expected distribution of sedimentary basins formed during intracratonic indentation.

## References

- Allen, J.R.L., and Banks, N.L. 1972. An interpretation and analysis of recumbent-folded deformed cross-bedding. *Sedimentology*, **19**: 257-283.
- Aspler, L.B., and Donaldson, J.A. 1985. The Nonacho Basin (Early Proterozoic), Northwest Territories, Canada: sedimentation and deformation in a strike-slip setting. *In* *Strike-Slip Deformation, Basin Formation, and Sedimentation*. Edited by: Biddle, K.T., and Christie-Blick, N. Society of Economic Paleontologists and Mineralogists, pp. 193-209.
- Bowring, S.A., Housh, T.B., and Isachsen, C.E. 1990. The Acasta gneisses: remnant of Earth's early crust. *In* *Origin of the Earth*. Edited by: Newsome, H., and Jones, J. Lunar and Planetary Institute, Houston, pp. 319-343.
- Bull, W.B. 1968. Alluvial fans. *Journal of Geological Education*, **16**: 101-106.
- Campbell, F.H.A., 1979. Stratigraphy and sedimentation in the Helikian Elu Basin and Hiukitak platform, Bathurst Inlet, Melville Sound, Northwest Territories. *Geological Survey of Canada Paper* 79-8. 18 p.
- Christie-Blick, N., and Biddle, K.T. 1985. Deformation and basin formation along strike-slip faults. *In* *Strike-Slip Deformation, Basin Formation and Sedimentation*. Edited by: Biddle, K.T., and Christie-Blick, N. Society of Economic Paleontologists and Mineralogists, pp. 1-34.
- DeCelles, P.G., Langford, R.P., and Schwartz, R.K. 1983. Two new methods of paleocurrent determination from trough cross-stratification. *Journal of Sedimentary Petrology*, **53**: 629-642.
- Dickinson, W.R. 1970. Interpreting detrital modes of graywacke and arkose. *Journal of Sedimentary Petrology*, **40**: 695-707.
- Dickinson, W.R., Beard, L.S., Brakenridge, G.R., Erjavec, J.L., Ferguson, R.C., Inman, K.F., Knepp, R.A., Lindberg, F.A., Ryberg, P.T. 1983. Provenance of North American Phanerozoic sandstones in relation to tectonic setting. *Geological Society of America Bulletin*, **94**: 222-235.
- Dickinson, W.R., and Suczek, C.A. 1979. Plate tectonics and sandstone compositions. *American Association of Petroleum Geologists Bulletin*, **63**: 2164-2182.

- Donaldson, J.A. 1965. The Dubawnt Group, Districts of Keewatin and MacKenzie. Geological Survey of Canada Paper 64-20, 11 p.
- Gandhi, S.S., and Loveridge, W.D. 1982. A Rb-Sr study of the Et-Then Group basalts, Great Slave Lake, District of Mackenzie. *In* Current Research, Part C. Geological Survey of Canada, pp. 155-160.
- Geological Survey of Canada. 1987. Magnetic anomaly map of Canada. 5th edition, Geological Survey of Canada, Map 1255A, scale 1:5,000,000
- Gibb, R.A., and Thomas, M.D. 1977. The Thelon Front: a cryptic suture in the Canadian Shield?. *Tectonophysics*, **38**: 211-222.
- Gibb, R.A. 1978. Slave-Churchill collision tectonics. *Nature*, **271**: 50-52.
- Grotzinger, J.P., and McCormick, D.S. 1987. Flexure of the early Proterozoic lithosphere and the evolution of Kilohigok basin (1.9 Ga), northwest Canadian shield. *In* New Perspectives in Basin Analysis. *Edited by*: Kleinspehn, K., and Paola, C. Springer-Verlag, Heidelberg, pp. 405-430.
- Haines, G.V., Hannaford, W., and Riddihough, R.P. 1971. Magnetic anomalies over British Columbia and the adjacent Pacific Ocean. *Canadian Journal of Earth Science*, **8**: 387-391.
- Hanmer, S. 1988. Geology, Great Slave Lake Shear Zone: parts of Fort Resolution, Snowdrift and Fort Reliance map areas, District of Mackenzie, NWT. Geological Survey of Canada Open-file 1783 1:100,000
- Hanmer, S., Bowring, S., van Breemen, O., and Parrish, R. 1992. Great Slave Lake shear zone, NW Canada: mylonitic record of Early Proterozoic continental convergence, collision and indentation. *Journal of Structural Geology*, **14**: 757-773.
- Hempton, M.R., and Dewey, J.F. 1983. Earthquake-induced deformational structures in young lacustrine sediments, East Anatolian Fault, southeast Turkey. *Tectonophysics*, **98**: T7-T14.

- Henderson, J.B., McGrath, P.H., Theriault, R.J., and van Breemen, O. 1990. Intracratonic indentation of the Archean Slave Province into the Early Proterozoic Thelon Tectonic Zone of the Churchill Province, northwestern Canadian Shield. *Canadian Journal of Earth Sciences*, **27**: 1699-1713.
- Hoffman, P.F. 1969. Proterozoic paleocurrents and depositional history of the East Arm Fold Belt, Great Slave Lake. *Canadian Journal of Earth Sciences*, **6**: 441-462.
- Hoffman, P.F. 1976. Environmental diversity of Middle Precambrian Stromatolites. *In* *Stromatolites*. Edited by: Walter, M.R. Elsevier Scientific Publishing Co., pp. 599-611.
- Hoffman, P.F. 1980. Wopmay orogen: a Wilson cycle of early Proterozoic age in the northwest of the Canadian shield. *In* *The Continental Crust and its Mineral Deposits*, Geological Association of Canada Special Paper 20. Edited by: Strangway, D.W. pp. 523-549.
- Hoffman, P.F. 1987. Continental transform tectonics: Great Slave Lake shear zone (ca. 1.9 Ga), northwest Canada. *Geology*, **15**: 785-788.
- Hoffman, P.F. 1988a. Geology and Tectonics, East Arm of Great Slave Lake, Northwest Territories, Map 1628, scale 1:250,000 and 1:500,000.
- Hoffman, P.F. 1988b. United plates of America, the birth of a craton: Early Proterozoic assembly and growth of Laurentia. *Annual Review of the Earth and Planetary Sciences*, **16**: 543-603.
- Hoffman, P.F. 1989. Precambrian geology and tectonic history of North America. *In* *The Geology of North America -- An overview*. Edited by: Bally, A.W., and Palmer, A.R. Geological Society of America, Boulder, Colorado, pp. 447-512.
- Hoffman, P.F., Bell, I.R., Hildebrand, R.S., and Thorstad, L. 1977. Geology of Athapuscow Aulacogen, East Arm, Great Slave Lake, District of MacKenzie. *In* *Report of Activities, Part A*; Geological Survey of Canada, Paper 77-1A, pp. 117-128.
- Hooke, R.L. 1967. Processes on arid region alluvial fans. *Journal of Geology*, **75**: 438-460.
- Hooke, R.L., and Rhorer, W.L. 1979. Geometry of alluvial fans: effect of discharge and sediment size. *Earth Surface Processes*, **4**: 147-166.

- Ingersoll, R.V., Bullard, T.F., Ford, R.L., Grimm, J.P., Pickle, J.D., and Sares, S.W. 1984. The effect of grain size on detrital modes: a test of the Gazzi-Dickinson point-counting method. *Journal of Sedimentary Petrology*, **54**: 103-116.
- Keunen, P.H. 1958. Experiments in geology. *Geological Magazine*, **23**: 1-28.
- LeCheminant, A.N., and Heaman, L.M. 1989. Mackenzie igneous events, Canadian Middle Proterozoic hotspot magmatism associated with ocean opening; *Earth and Planetary Science Letters*, **96**: pp. 38-48.
- Loveridge, W.D., Eade, K.E., and Sullivan, R.W. 1988. Geochronological studies of Precambrian rocks from the southern District of Keewatin. Geological Survey of Canada Paper 88-18.
- Miall, A.D. 1978. Lithofacies types and vertical profile models in braided river deposits: a summary. *In* *Fluvial Sedimentology*. Edited by: Miall, A.D. Canadian Society of Petroleum Geologists, Calgary, pp. 597-604.
- McCormick, D.S., and Grotzinger, J.P. 1992. Evolution and significance of an overfilled alluvial foreland basin: Burnside Formation (1.9 Ga), Kilohigok basin, N.W.T., Canada. *Basin Research*, **4**: 253-278.
- McKenzie, D. 1972. Active tectonics of the Mediterranean region. *Geophysical Journal of the Royal Astronomical Society*, **30**: 109-185.
- Molnar, P. and Tapponnier, P. 1975. Cenozoic tectonics of Asia: effects of a continental collision. *Science*, **189**: 419-426.
- Molnar, P. and Tapponnier, P. 1977. Relation of the tectonics of eastern China to the India-Eurasia collision: application of slip-line field theory to large-scale continental tectonics. *Geology*, **5**: 212-216.
- Pelechaty, S.M., and James, N.P. 1991. Dolomitized Middle Proterozoic calcretes, Bathurst Inlet, Northwest Territories, Canada. *Journal of Sedimentary Petrology*, **61**: 988-1001.

- Picard, M.D., and High, L.R. 1981. Physical stratigraphy of ancient lacustrine deposits. *In* Recent and Ancient Nonmarine Depositional Environments. *Edited by:* Ethridge, F.G., and Flores, L.R. Society of Economic Paleontologists and Mineralogists Special Publication number 31, pp. 233-260.
- Ridgway, K.D., and DeCelles, P. G. 1993. Petrology of mid-Cenozoic strike-slip basins in an accretionary orogen, St. Elias Mountains, Yukon Territory, Canada. *In* Processes Controlling the Composition of Clastic Sediments. *Edited by:* Johnsson, M.J., and Basu, A. Geological Society of America, pp. 67-89.
- Ritts, B.D. 1994. The sedimentology and provenance of the Et-Then Group as a record of deformation on the McDonald fault zone, East Arm, Great Slave Lake, Northwest Territories. *In* Current Research 1994-C. Geological Survey of Canada, pp. 39-48.
- Ross, G.M., Parrish, R.R., Villeneuve, M.E., and Bowring, S.A. 1991. Geophysics and geochronology of the crystalline basement of the Alberta Basin, western Canada. *Canadian Journal of Earth Science*, 28: 512-522.
- Rust, B.R. 1978. Depositional models for braided alluvium. *In* Fluvial Sedimentology. *Edited by:* Miall, A.D. Canadian Society of Petroleum Geologists, Calgary, pp. 605-626.
- Sims, J.D. 1973. Earthquake-induced structures in sediments of Van Norman Lake, San Fernando, California. *Science*, 182: 161-163.
- Sims, J.D. 1975. Determining earthquake recurrence intervals from deformational structures in young lacustrine sediments. *Tectonophysics*, 29: 141-152.
- Stockwell, C.H. 1936. East Arm of Great Slave Lake; Geological Survey of Canada, Map 377A and 378A (with descriptive notes).
- Tapponnier, P. and Molnar, P. 1976. Slip line field theory and large scale continental tectonics. *Nature*, 264: 319-324.
- Theriault, P., and Desrochers, A. 1993. Carboniferous calcretes in the Canadian Arctic. *Sedimentology*, 40: 449-465.



Thomas, M.D., Gibb, R.A., and Quince, J.R. 1976. New evidence from offset aeromagnetic anomalies for transcurrent faulting associated with the Bathurst and McDonald faults, Northwest Territories. *Canadian Journal of Earth Science*, **13**: 1244-1250.

Tirrul, R., and Grotzinger, J.P. 1990. Early Proterozoic collisional orogeny along the northern Thelon tectonic zone, Northwest Territories, Canada: evidence from the foreland. *Tectonics*, **9**: 1015-1036.

**Table 1. Summary, Proterozoic sedimentary, igneous, structural and age information in Athapuscow basin**

Stratigraphy	Igneous events	Deformation episodes	Geochronology
	MacKenzie Dikes		1270 Ma. <sup>1</sup>
	Fortress Gabbro dikes		
<b>Et-Then Group</b>	minor basalt flows	<b>McDonald Fault System</b>	
	Compton Laccoliths		1865 Ma. <sup>2</sup>
		East Arm fold and thrust belt	
Christie Bay Group	basalt		
Pethei Group			
	gabbro intrusions		
Kahochella Group	basalt/rhyolite		
Sosan Group and Wilson Island Group			1928- ?? Ma. <sup>2</sup>
		Great Slave Lake shear zone	1970-1930 Ma. <sup>3</sup>
	Thelon-Taltson magmatic arc		2050-1920 Ma. <sup>3</sup>
<b>Union Island Group</b>	basalt	normal faulting	
	Hearne Dikes		??
	Blachford intrusive suite, late phase		2085 Ma. <sup>2</sup>
	Blachford intrusive suite, early phase		2170 Ma. <sup>2</sup>
	Simpson Island dike		
	Archean crystalline basement		>2550 Ma. <sup>4</sup>

a/c

a/c

n/c

The Great Slave Supergroup consists of the Sosan, Kahochella, Pehtei and Christie Bay groups. Geochronology sources are: <sup>1</sup>LeCheminant and Heaman (1989); <sup>2</sup>Bowring et al (1984); <sup>3</sup>Hanmer et al (1992); <sup>4</sup>Ross et al (1991). Table adapted from Hoffman et al (1977). n/c, nonconformity; a/c, angular unconformity.

<b>Table 2. Raw clast count data</b>						
<b>Section</b>	<b>Sample</b>	<b>Strat. level</b>	<b>Quartzite</b>	<b>Shale</b>	<b>Carbonate</b>	<b>Crystalline</b>
Snowdrift	CC1	top of Em	97	3		
<b>Murky Channel</b>						
	1MRK0	0 m	65	31	4	
	1MRK23	23 m	20	87	13	
	1MRK82	82 m	23	70	3	
	1MRK186	186 m	11	89		
	1MRK349	349 m	19	81		
	CC6	611 m	82	13	5	
	CC7	800 m	81	19		
	CC8	960 m	93	6	1	
<b>Et-Then ls.</b>						
	1ET1	1 m	80	18		
	1ET23	23 m	59	38	2	
	1ET60	60 m	84	14	1	
	1ETup9	69 m	90	10		
	2ET55	124 m	70	18	2	
	2ET80	149 m	70	20		
	2ET106	175 m	90	10		
<b>Preble ls.</b>						
	1PI0		48	38		6
	1PI21		34	3	52	11
	1PI48		29	7		63
	1PI102		26	0	58	16
	1Plup118		8			93
	STA 8		7			89
	STA 9		7			93
	1PItop2		14			76
	1PItop117		2			97
	1PItop271		2			94

**Note: stratigraphic level is measured from the base of the Murky Formation**

**Table 3. Point-Counting Parameters**

Code	Definition
Qmu	Undulose, monocrystalline quartz
Qmnu	Non-undulose, monocrystalline quartz
Qp	Polycrystalline quartz
Cht	Chert
P	Plagioclase feldspar
K	Potassium feldspar
Lv	Volcanic/hypabyssal lithic grains
Lmh	High-grade metamorphic grains; foliated quartz-mica aggregates
Lml	Low-grade metamorphic grains; foliated, illite-rich, fine grained
Ls	Sedimentary lithic grains: shale, siltstone
Lu	Unidentified lithic grain
M	Phyllosilicates
Qm	Monocrystalline quartz (Qmu+Qmnu)
Q	Quartzose grains (Qm+Qp+Cht)
F	Feldspar (P+K)
L	Labile lithic grains (Lv+Lmh+Lml+Ls+Lu)
Lt	Lithic grains (L+Qp+Cht)
$QFL\%Q = 100Q/(Q+F+L)$ $QFL\%F = 100F/(Q+F+L)$ $QFL\%L = 100L/(Q+F+L)$ $QmFLt\%Qm = 100Qm/(Qm+F+Lt)$ $QmFLt\%F = 100F/(Qm+F+Lt)$ $QmFLt\%Lt = 100Lt/(Qm+F+Lt)$ $P/F = P/F$	

Table 4. Sandstone Composition Data

Location	Fm	sample	Ornu	Ornuu	Op	Chl	P	K	Lv	Lmh	Unit	La	Lu	M	Total	On	F	Li	Qt	F	L	P/F	
Murky Channel	Ep	1SM1	240	77	3	0	77	32	11	0	1	5	3	1	450	317	109	24	320	109	21	766	
	Ep	2SM2	248	59	4	2	58	70	19	2	5	6	3	0	450	308	98	44	314	98	38	286	
	Ep	3SM1	248	64	1	0	51	66	5	0	0	9	6	0	450	312	117	21	313	117	20	436	
	Ep	4SM1	252	62	1	0	64	52	7	1	0	3	6	2	450	314	116	20	315	116	19	436	
	Ep	5SM1	335	56	1	0	24	23	1	1	0	3	6	0	450	391	47	12	392	47	11	552	
	Ep	6SM1	237	50	3	0	59	68	11	2	3	8	7	2	450	287	127	36	290	127	33	465	
	Ep	7SM35	221	100	7	2	21	57	16	4	4	9	8	2	450	321	78	51	330	78	42	269	
	Ep	8SM1	233	33	3	2	45	92	13	2	1	13	5	8	450	266	137	47	271	137	12	328	
	Ep	9SM1	285	57	4	0	24	65	3	0	0	4	4	1	450	342	89	19	349	89	12	270	
	Ep	10SM1	243	54	7	0	38	61	20	0	5	9	15	1	450	297	99	54	301	99	50	384	
	Ep	11SM1	233	62	4	0	57	73	5	0	1	6	7	3	450	295	127	28	299	127	34	425	
	Ep	12SM1	254	55	5	0	37	62	19	1	3	8	8	0	450	309	99	42	314	99	37	374	
	Ep	13SM1	269	49	5	2	24	65	18	0	1	7	9	1	450	318	89	43	325	89	36	270	
	Ep	14SM1	285	57	4	0	37	76	2	0	0	2	2	0	450	322	113	15	326	113	11	327	
	Ep	15SM1	289	58	4	0	40	60	3	2	0	7	8	0	450	327	100	23	330	100	20	400	
Ep	16SM1	285	76	3	1	9	51	7	0	1	4	7	3	450	371	60	19	375	60	15	150		
Ep	17SM1	222	74	3	1	40	43	4	0	0	4	12	7	1	450	346	83	21	351	83	16	482	
South of Basile Bay	Ep	2MCA	216	51	3	2	56	84	13	1	4	12	5	0	450	267	140	43	272	140	38	400	
	Ep	2MCA12	222	59	2	0	37	109	7	1	2	6	5	0	450	281	146	23	283	146	21	253	
	Ep	2MCA3	292	69	5	1	52	78	13	16	3	7	4	0	450	271	130	49	277	130	43	400	
	Ep	2MCA8	236	63	0	1	42	90	6	0	0	5	4	1	450	299	108	19	300	108	18	318	
	Ep	2MCA11	284	60	6	1	23	83	6	0	2	4	1	0	450	324	108	20	331	108	13	217	
	Ep	2MCA12	238	55	4	3	37	77	10	2	6	17	1	2	0	451	292	114	44	300	114	37	325
	Ep	2MCA17	245	47	4	4	44	89	4	0	6	8	5	0	450	293	133	25	300	133	17	331	
	Ep	2MCA19	270	66	2	0	37	69	2	0	0	2	2	2	0	450	336	106	8	338	106	6	349
	Ep	2MCA170	255	49	2	0	44	78	4	0	0	14	3	1	450	304	122	24	306	122	22	361	
	Ep	2MCA182	238	54	4	1	26	94	16	1	4	9	3	0	450	292	120	38	297	120	33	217	
	Ep	2MCA194	269	58	3	0	22	82	4	0	0	5	6	1	450	327	104	19	330	104	16	212	
	Ep	2MCA209	239	61	6	1	51	74	2	3	1	7	5	0	450	300	125	25	307	125	18	408	
	Ep	2MCA233	240	45	6	1	52	83	7	0	3	3	11	0	450	285	135	30	292	135	23	385	
	Ep	2MCA258	234	59	3	1	57	80	3	0	0	7	6	0	450	293	137	20	297	137	16	416	
	Ep	2MCA285	232	63	2	4	57	74	7	1	1	4	3	0	450	295	131	24	301	131	18	435	
Ep	2MCA305	251	51	4	2	43	81	1	3	0	7	7	0	450	302	124	24	308	124	18	347		
Ep	2MCA318	209	47	1	1	70	108	6	0	0	6	2	0	450	256	178	16	258	178	14	393		
Ep	2MCA333	214	44	2	0	64	113	4	1	1	3	8	2	0	450	254	177	19	256	177	17	362	
Ep	2MCA347	259	34	4	0	48	82	4	3	0	8	5	2	0	450	293	130	27	297	130	23	369	
Ep	2MCA363	228	38	5	2	61	97	5	0	0	9	5	0	450	266	158	26	273	158	19	386		
Ep	2MCA387	226	33	9	2	70	87	4	1	0	7	10	1	450	259	157	34	270	157	23	446		
Ep	2MCA433	229	39	3	2	47	102	4	4	0	9	11	0	450	268	149	33	273	149	28	315		
Ep	2MCA449	232	22	7	0	49	118	2	0	0	10	8	2	450	254	167	29	261	167	22	293		
Ep	2MCA505	216	63	4	0	40	105	2	0	2	8	10	0	450	279	145	26	283	145	22	278		
Et-Then Island	Ep	3MCS	233	52	2	1	54	84	12	2	1	4	1	0	450	285	138	27	288	138	24	391	
	Ep	2ET140	249	47	2	0	23	98	5	1	1	11	13	0	450	296	121	33	298	121	31	190	
	Ep	2ET167	285	70	1	1	18	78	4	0	0	6	6	1	450	335	96	19	337	96	17	188	
	Ep	3ET14	236	64	1	1	40	98	2	0	0	4	4	0	450	300	138	12	302	138	10	290	
	Ep	3ET16	279	46	4	2	45	58	3	0	0	7	6	0	450	325	103	22	331	103	16	437	
	Ep	3ET177	237	62	2	0	33	82	3	4	1	12	11	1	450	299	115	36	303	115	32	287	
	Ep	3ET196	234	72	1	0	21	74	12	3	5	17	10	1	450	306	95	49	307	95	48	281	
	Ep	3ET130	246	56	4	0	17	97	7	3	5	12	4	1	450	302	114	34	306	114	30	347	
	Ep	3ET142	232	51	4	1	58	81	7	0	0	8	8	0	450	283	139	28	288	139	23	417	
	Ep	3ET193	207	53	1	2	57	100	8	3	2	6	10	1	450	260	157	33	263	157	30	363	
	Ep	3ET198	240	64	4	0	35	79	1	1	4	7	13	2	450	304	114	32	308	114	28	307	
	Ep	3ET215	278	78	0	0	18	59	3	1	1	8	5	0	450	356	77	17	356	77	17	234	
	Ep	3ET228	260	50	4	0	47	50	2	0	1	10	6	0	450	330	97	23	334	97	19	485	
	Ep	3ET279	213	57	2	3	59	105	0	1	0	2	8	0	450	270	164	16	275	164	11	360	
	Ep	3ET335	240	43	3	1	0	115	5	0	0	31	11	1	450	283	115	52	287	115	48	0	

Preble Island	Ep	3ET345	307	33	1	1	4	87	2	0	0	10	4	1	450	340	91	19	342	91	17	044
	Ep	3P12	209	37	3	2	90	78	7	1	1	8	10	4	450	246	168	36	251	168	31	.536
	Ep	3P13	190	33	5	0	84	96	5	1	5	16	14	1	450	223	180	47	228	180	42	.467
	Ep	3P14	202	60	3	4	70	84	7	2	2	7	10	1	450	262	154	34	269	154	27	.455
	Ep	3P15	222	29	6	3	82	76	11	3	2	5	7	2	450	251	158	41	260	158	32	.519
	Ep	3P16	222	17	4	2	78	92	8	2	1	16	5	1	450	239	171	40	245	171	34	.462
	Ep	3P17	221	22	2	2	70	113	5	2	0	8	5	0	450	243	183	32	247	183	29	.383
	Ep	3P18	226	21	2	1	76	95	11	2	3	2	10	0	450	247	171	32	250	171	29	.444
	Ep	3P19	257	33	3	5	52	80	6	1	0	4	9	0	450	290	132	28	298	132	20	.394
	Ep	3P110	205	45	9	0	79	91	6	1	0	10	4	0	450	250	170	30	259	170	21	.465
	Ep	1P1601	193	25	4	0	129	53	14	2	4	12	11	3	450	218	182	50	222	182	46	.709
	Ep	1P1602	255	30	3	1	80	50	4	0	2	8	13	4	450	285	130	35	289	130	31	.615
	Ep	1P1605/2	193	18	3	0	108	99	4	3	1	11	6	4	450	211	207	32	214	207	29	.522
Island near Snowditt	Ep	3ANNE	295	31	5	1	42	66	2	1	0	3	4	2	450	326	108	16	322	108	10	.389
	Ep	4ANNE	262	62	3	0	24	59	7	7	4	12	8	2	450	324	83	43	327	83	40	.289
	Ep	6ANNE	258	24	2	0	95	78	5	1	5	14	8	1	450	240	173	37	244	173	33	.549
	Ep	1RC7	240	66	5	0	81	65	2	0	1	7	9	1	450	282	146	22	284	146	20	.555
	Em	1RC41	250	94	1	0	5	39	6	2	5	63	19	0	450	306	44	100	311	44	95	.114
	Em	1RC54	242	101	2	0	14	21	5	1	7	38	8	1	450	344	35	71	345	35	70	.400
	Em	1RC74	261	78	3	1	7	38	6	0	1	37	12	1	450	343	45	62	348	45	57	.156
	Em	1RC85	285	89	1	1	9	20	1	2	0	26	9	0	450	339	69	42	343	69	38	.101
	Em	1RC98	227	90	5	4	6	59	6	2	4	36	10	1	450	317	65	68	326	65	59	.092
	Em	1RC121	261	72	2	0	10	38	5	1	1	53	7	0	450	333	48	69	335	48	67	.208
	Em	1RC132	280	55	5	2	3	66	4	1	0	24	9	1	450	335	69	46	342	69	39	.043
	Em	1RC187	298	38	5	1	4	65	5	4	1	14	14	1	450	336	69	45	342	69	39	.058
	Em	1RC201	323	38	6	2	5	50	3	0	0	13	10	0	450	361	55	34	369	55	26	.081
	Em	2RC3	286	37	1	1	2	55	4	4	3	38	16	3	450	323	57	70	325	57	68	.035
	Em	2RC23	280	30	3	1	4	83	1	0	0	33	15	1	451	310	87	54	314	87	50	.046
	Em	2RC92	302	33	5	0	3	68	1	1	3	13	18	3	450	335	71	44	340	71	39	.042
Et-Twen Island	Em	1ET3	213	106	3	1	10	77	5	1	2	22	10	0	450	319	87	44	323	87	40	.115
	Em	2ET10	178	82	5	8	7	90	4	0	3	49	24	0	450	260	97	93	273	97	80	.072
	Em	2ET29	203	59	5	5	4	105	5	0	5	41	24	2	450	262	109	79	272	109	69	.037
	Em	2ET53	115	65	2	5	1	58	4	1	2	89	17	1	360	180	59	121	187	59	114	.017
	Em	2ET83	162	28	4	0	3	48	6	2	6	113	29	0	401	190	51	160	194	51	156	.059
Island near Snowditt	Em	1NNE	266	18	4	0	2	104	5	1	1	32	13	4	450	284	106	60	288	106	56	.019
	Em	2NNE	216	62	1	0	25	87	7	3	3	36	10	2	450	278	112	60	279	112	59	.223
	Em	END	371	28	11	1	0	0	2	2	2	22	10	1	450	399	0	51	411	0	39	.389
	Em	EM8	199	11	2	0	74	116	4	0	0	26	16	2	450	210	190	50	212	190	48	.389
	Em	EM4	117	29	4	0	34	65	18	1	2	27	17	2	316	146	99	71	150	99	67	.343
	Em	1P161	282	43	4	2	3	58	7	2	5	25	15	4	450	325	81	64	331	61	58	.341
	Em	1P165	280	25	5	0	28	54	5	4	4	23	24	2	450	305	82	63	310	82	58	.049
	Em	1P167A	234	44	5	1	61	43	13	3	1	4	14	7	450	278	124	48	284	124	42	.653
	Em	1P168	279	33	5	0	47	60	12	2	0	2	10	0	450	312	107	31	317	107	26	.439
	Em	1P169	212	24	4	1	68	84	7	3	1	4	8	1	450	236	182	32	240	182	28	.538
	Em	1P169a	233	52	4	0	95	69	4	4	4	8	11	2	450	285	134	32	240	134	26	.485
	Em	1P169b	257	25	2	0	84	43	11	3	3	7	12	5	450	282	127	41	284	127	39	.661
	Em	1P169c	237	34	5	2	80	60	5	3	6	6	15	0	450	271	140	39	276	140	32	.571
	Em	1P169d	236	38	3	0	91	52	2	5	4	4	13	3	450	274	143	33	277	143	30	.636

---

---

**Table 5. Evidence in the Et-Then Group for Intracratonic Indentation Tectonics**

---

<b>Criterion</b>	<b>Description</b>
<b>Formation and Member Thickness</b>	The Murky Formation thins from over 1000 m near the McDonald fault to less than 300 m at Et-Then Island, on the northwest side of the Et-Then basin. The shale-clast conglomerate "member" thins from over 400 m in the southeast to zero at Et-Then Island in the northwest. Preble Formation thickness is relatively uniform over the basin.
<b>Facies Trends and Depositional Systems</b>	Murky Formation alluvial fan facies become more distal to the northwest, away from the McDonald fault. The Preble Formation is a sandy braided fluvial deposit over the entire basin.
<b>Paleocurrent Trends</b>	Murky Formation paleocurrents are directed to the northwest, away from the McDonald fault. Preble Formation paleocurrents are directed to the west southwest, parallel to the McDonald fault and away from the apex of the Slave indenter.
<b>Compositional Trends</b>	Murky Formation sediments largely are derived from sedimentary, local East Arm lithologies. Preble Formation sediments are derived from granitoid rocks (some mylonitic); probably from the apex of the indenter.
<b>Textural Trends</b>	Murky Formation mainly consists of cobble to boulder conglomerate and fines to the northwest away from the McDonald fault. Preble Formation consists almost entirely of sandstone and shows no discernible lateral textural trends.

---

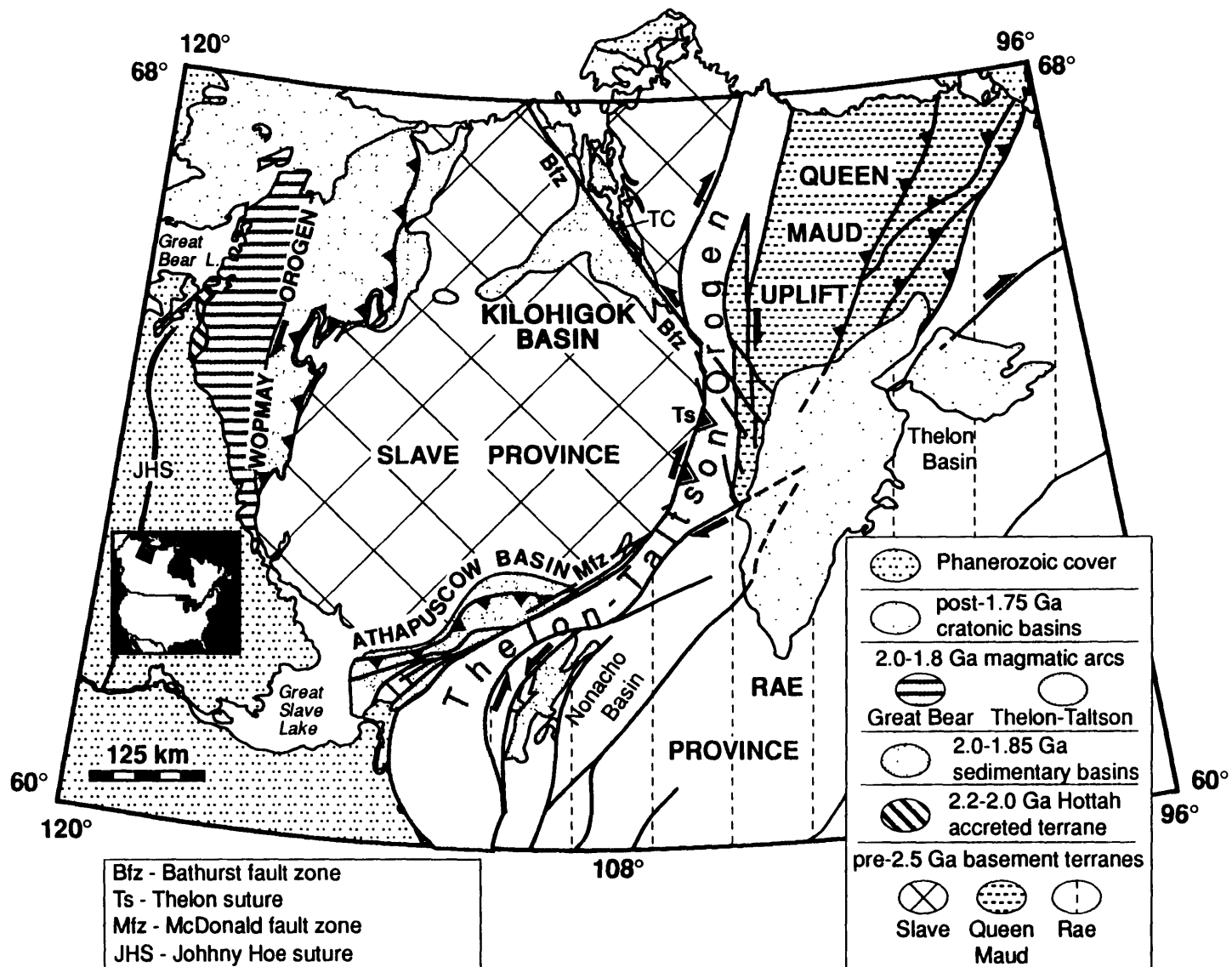


Figure 1



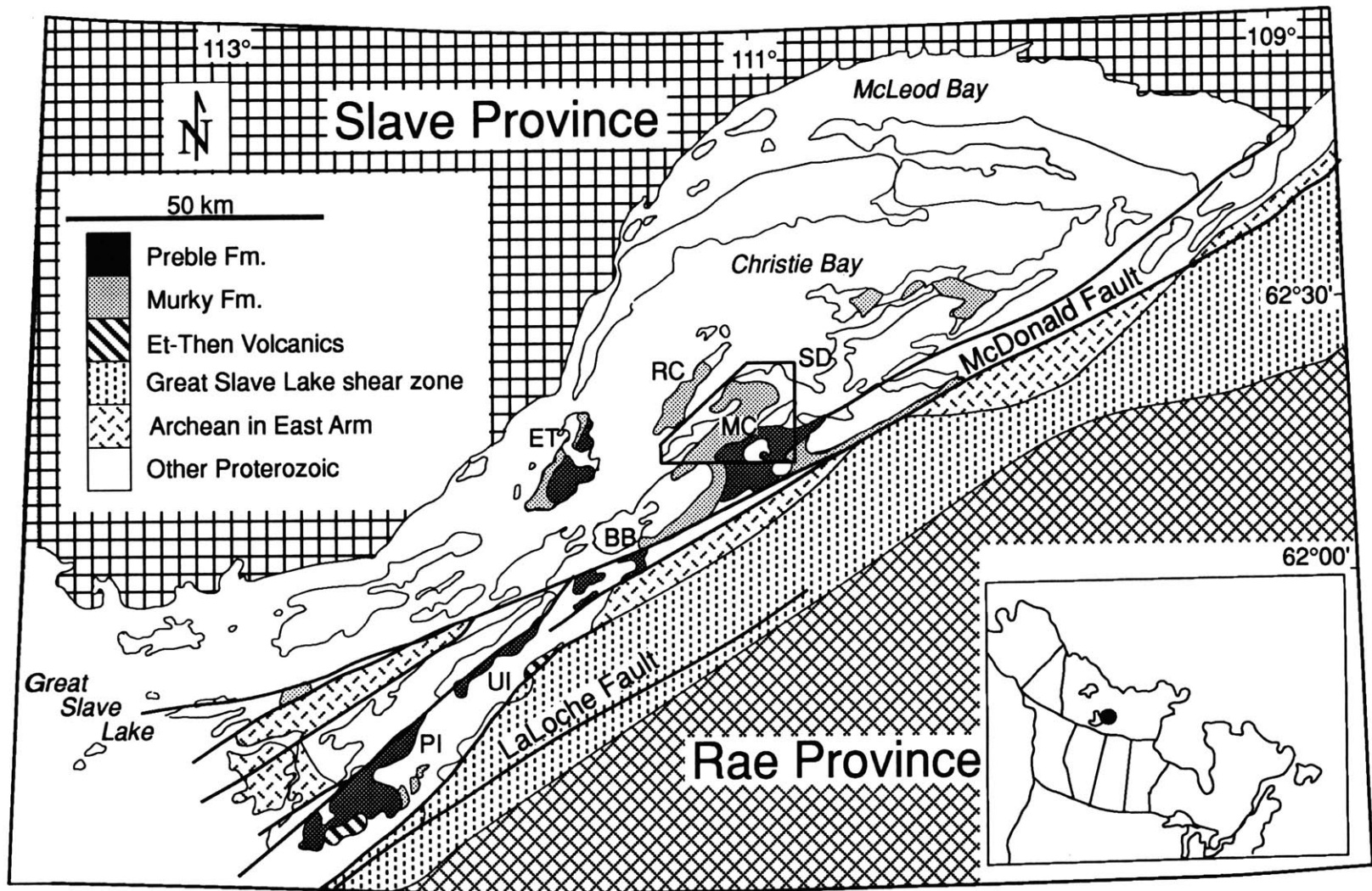


figure 2

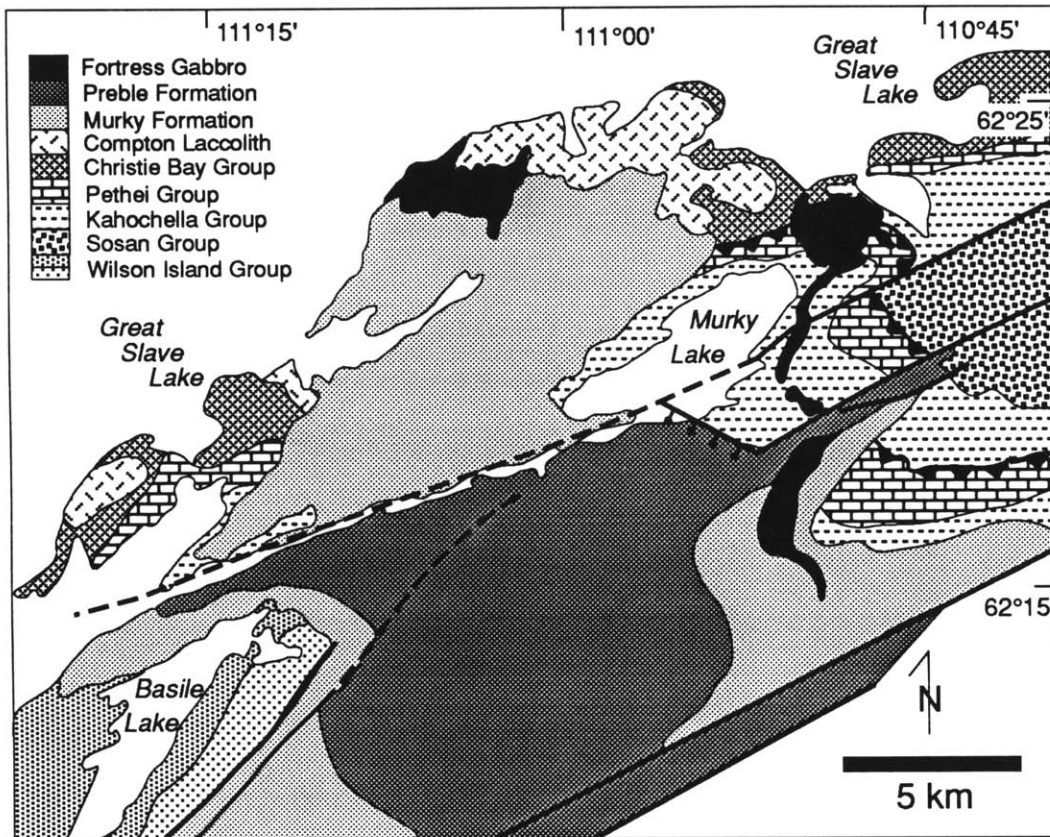


figure 3

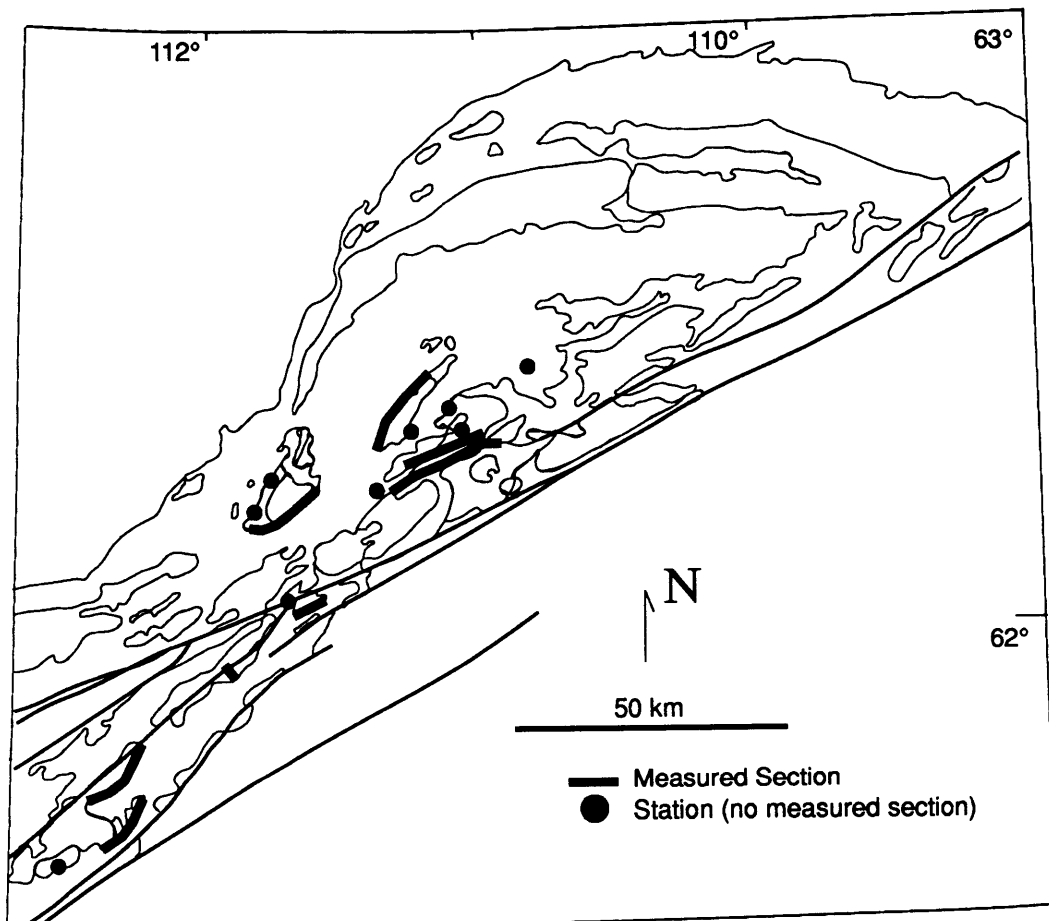


figure 4

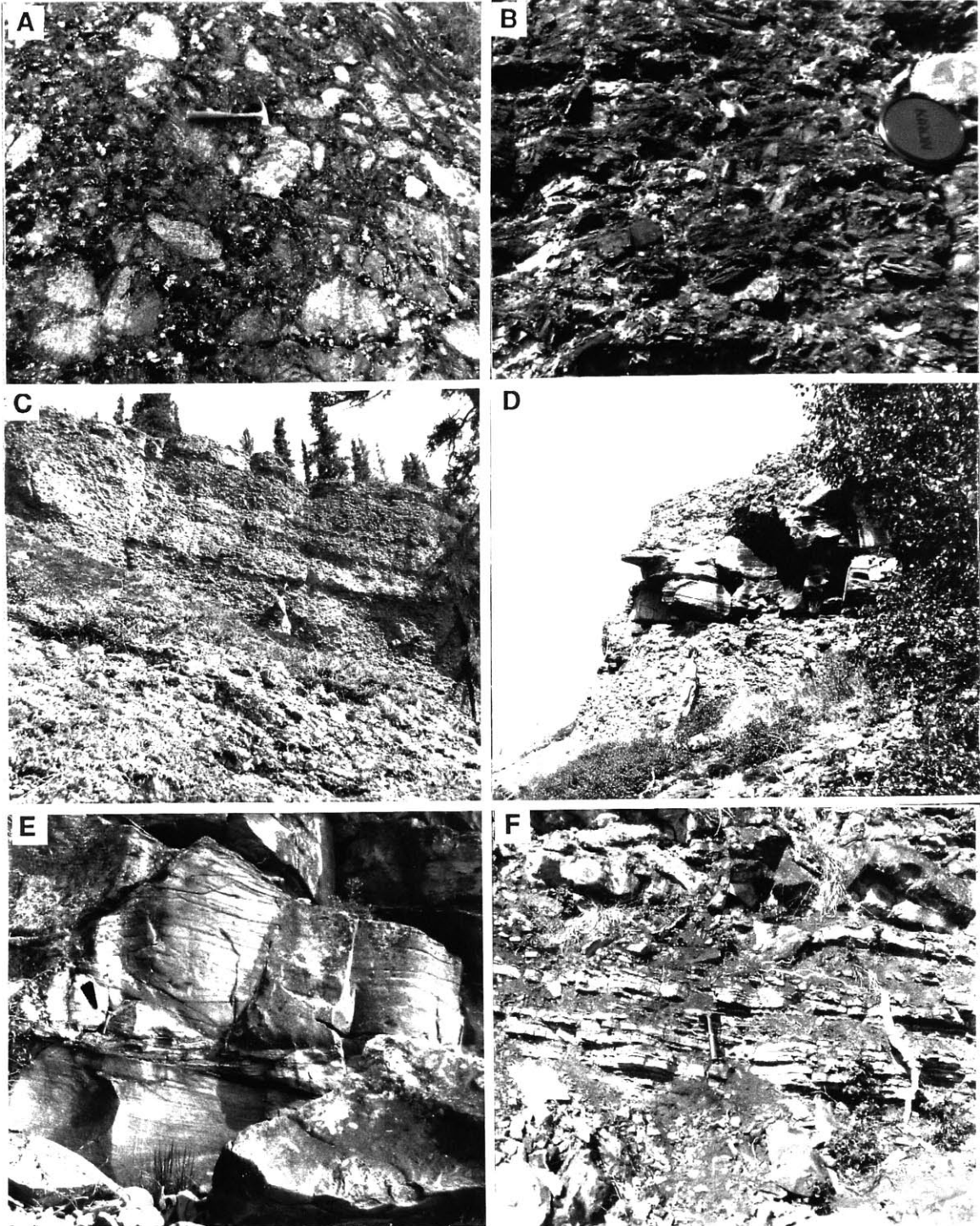
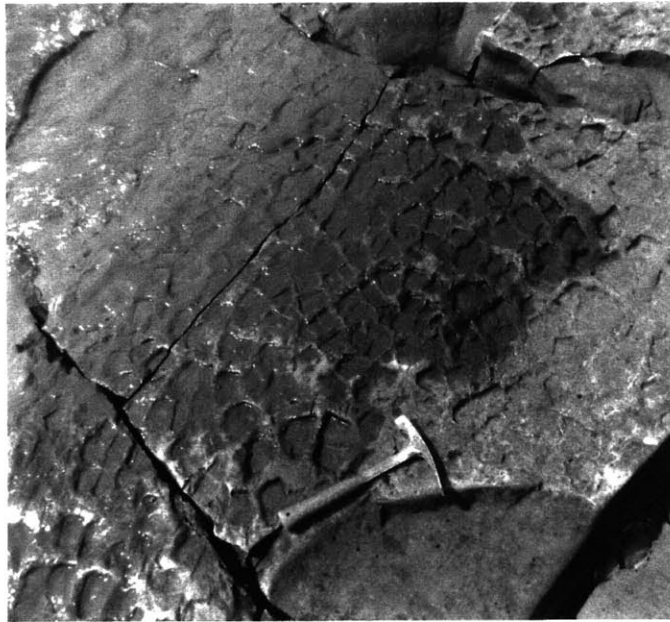
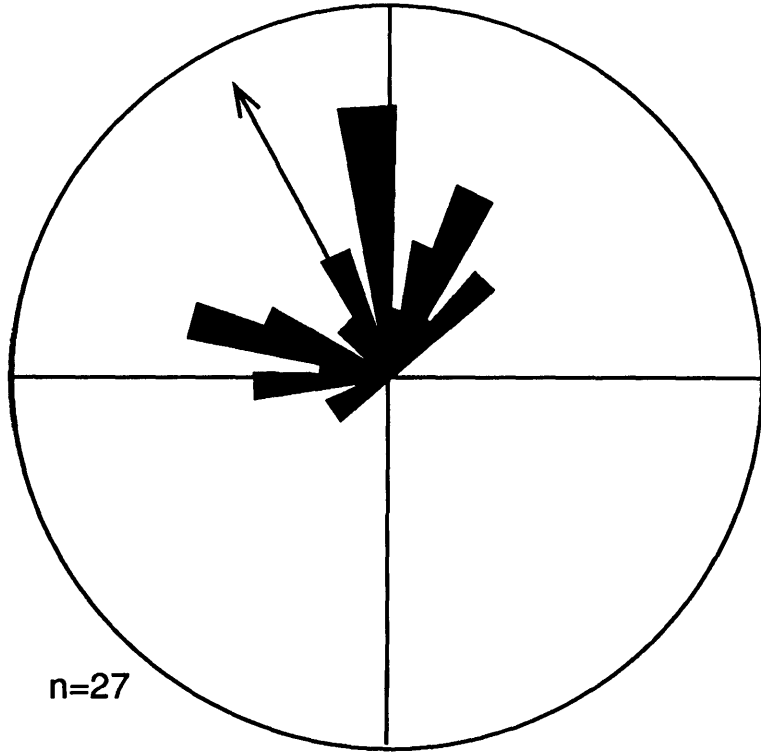


figure 5



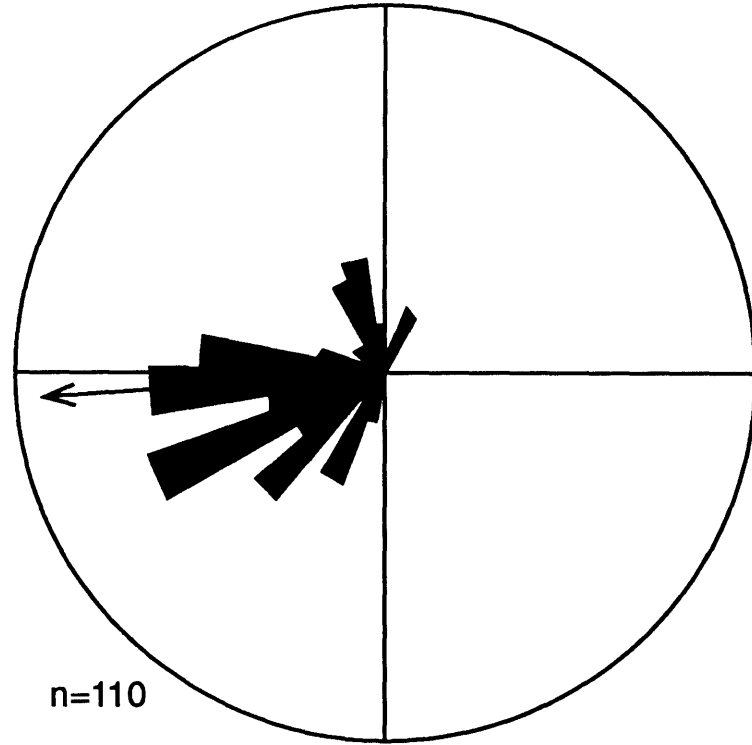
**figure 6**





n=27

Murky Formation  
(a)



n=110

Preble Formation  
(b)

figure 8

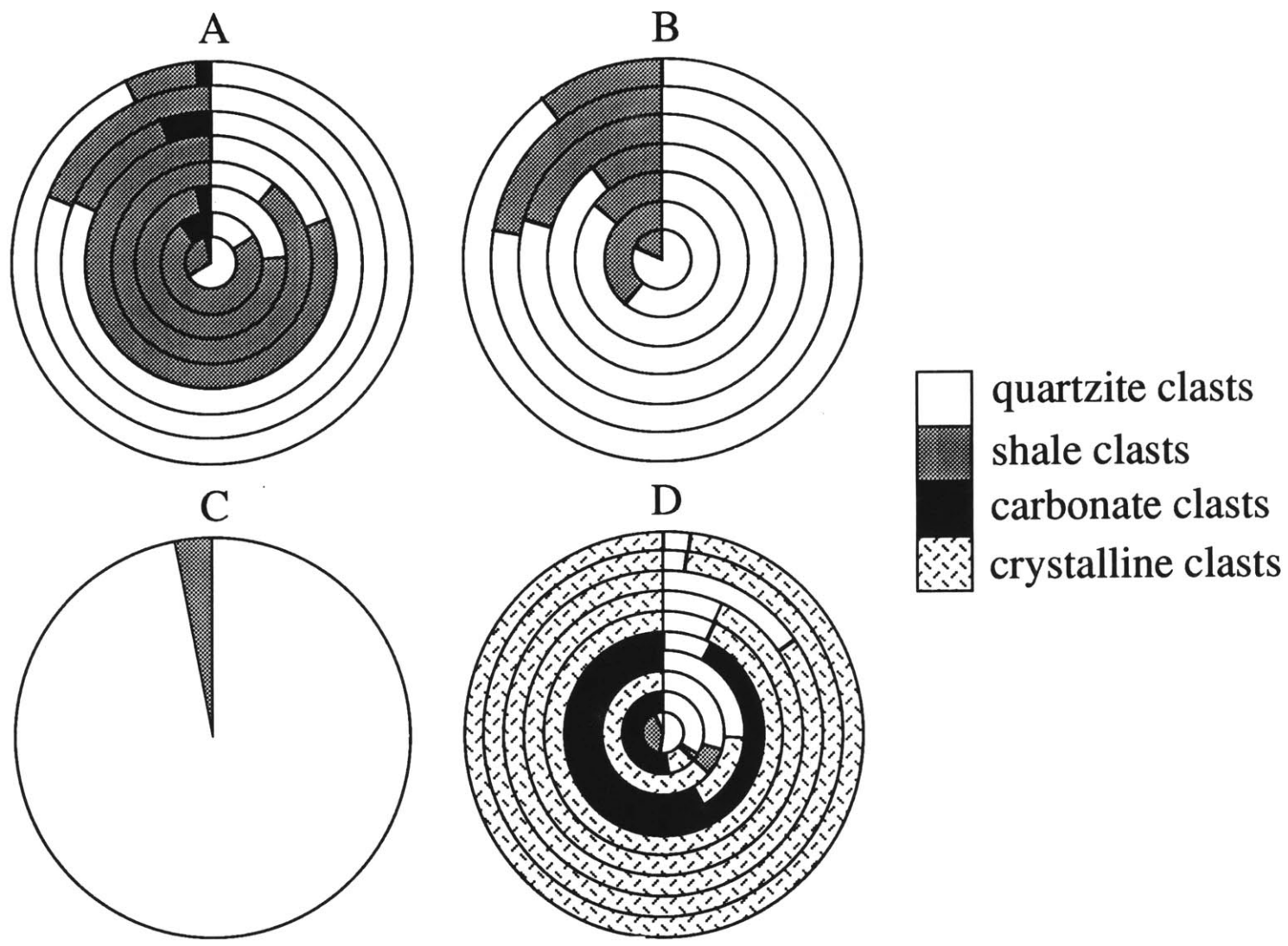


figure 9



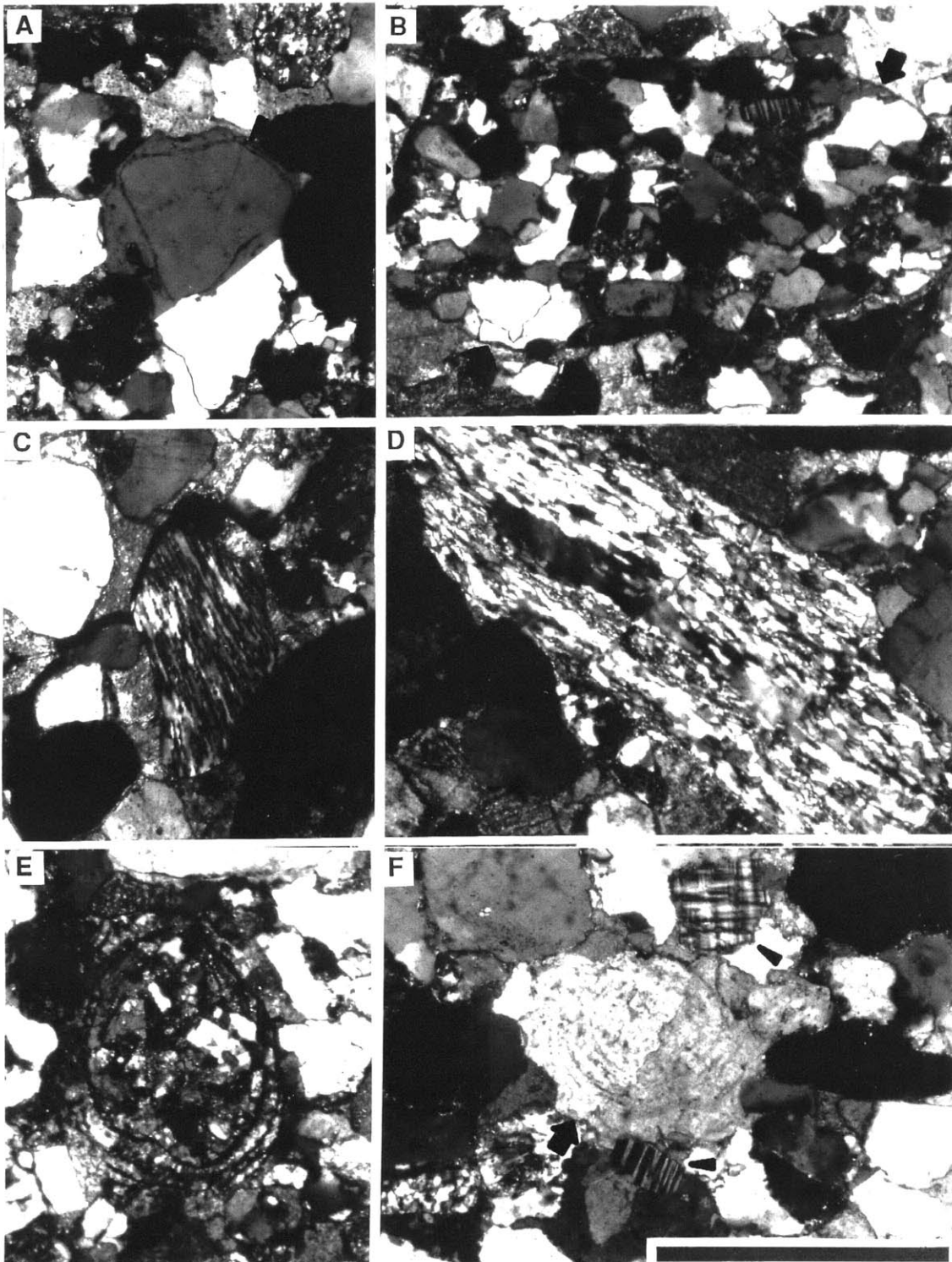


figure 10

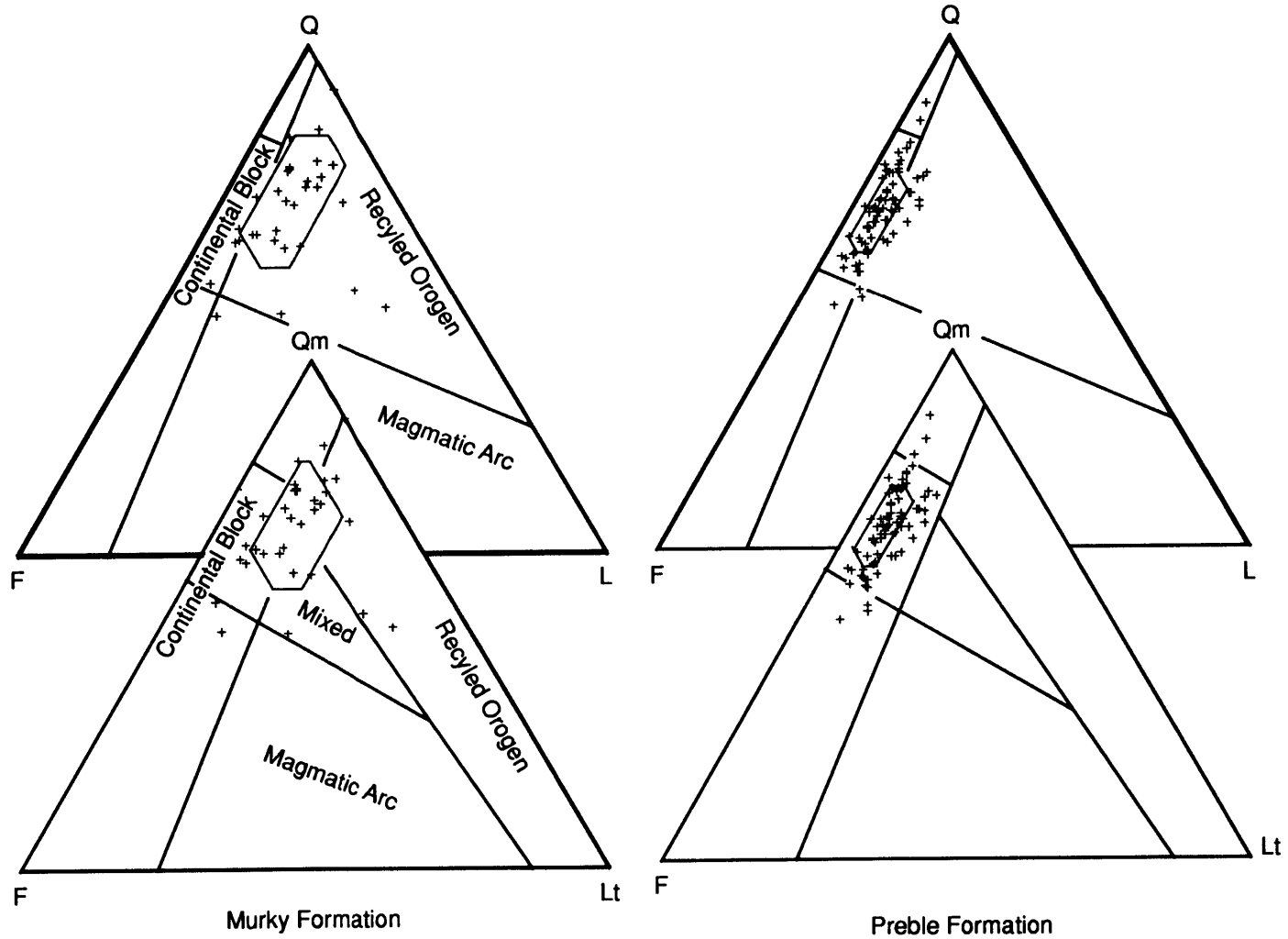


figure 11

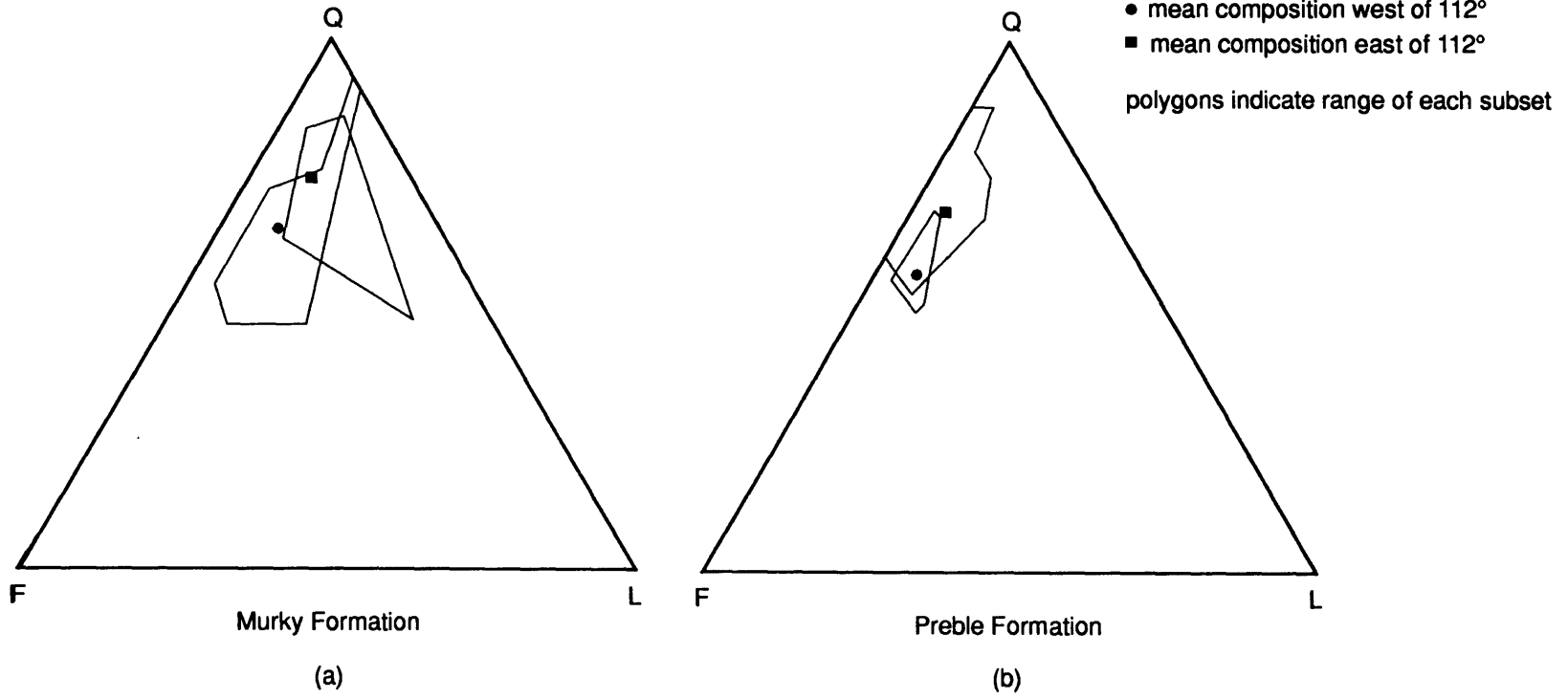


figure 12

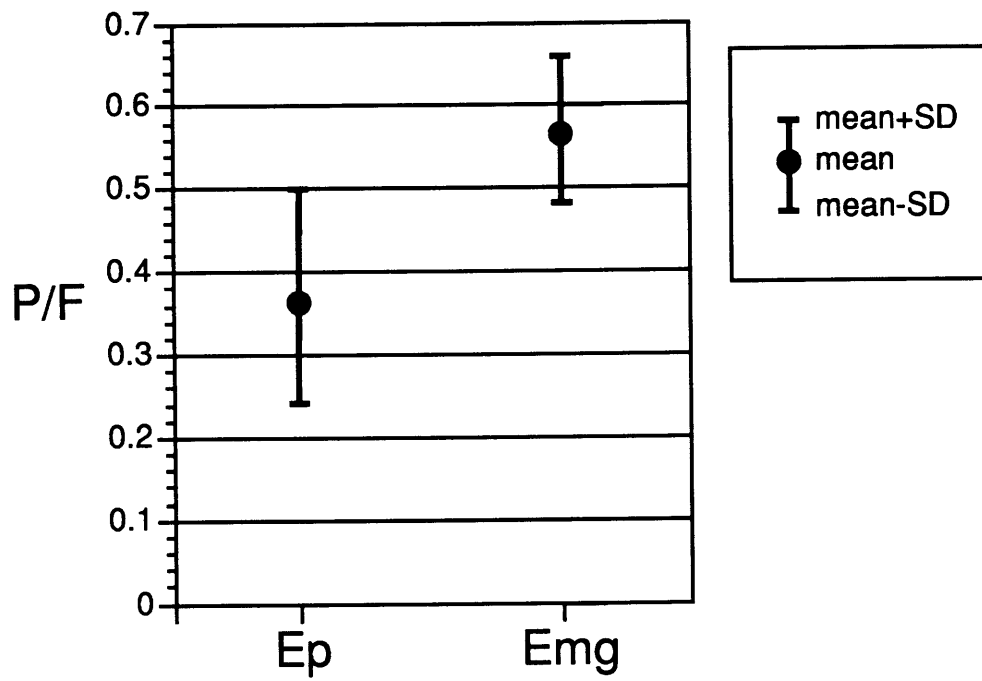


figure 13

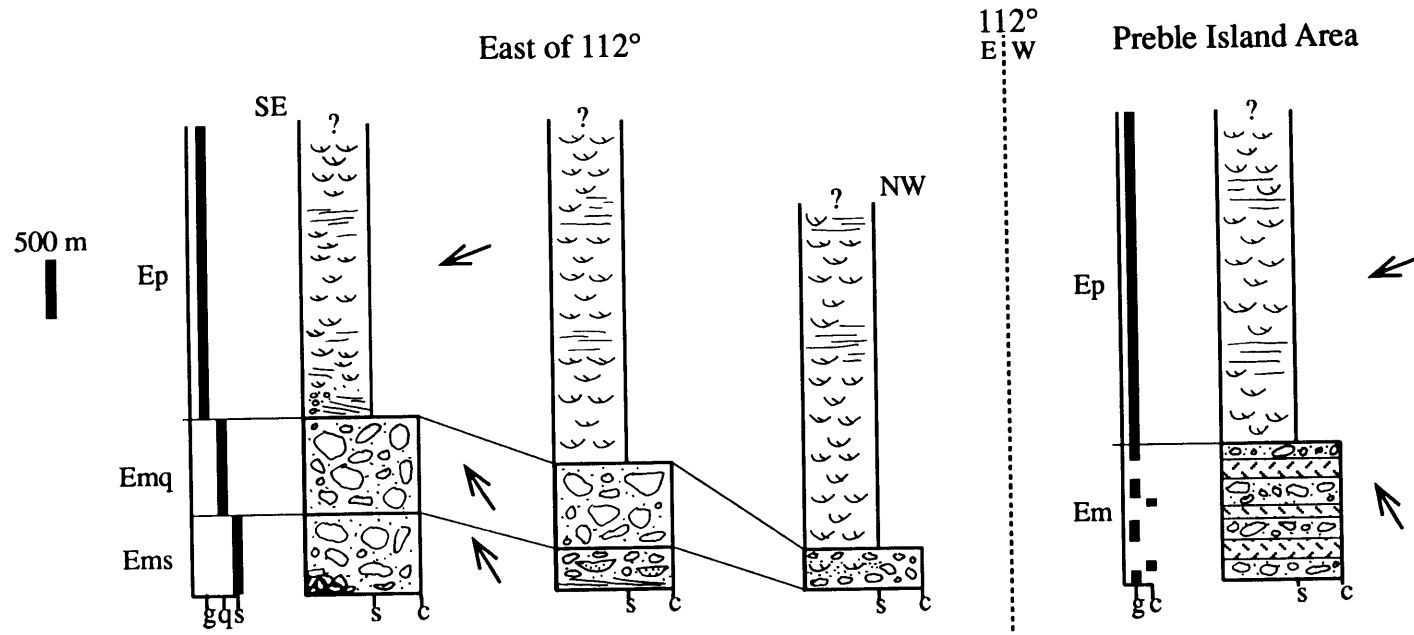


figure 14

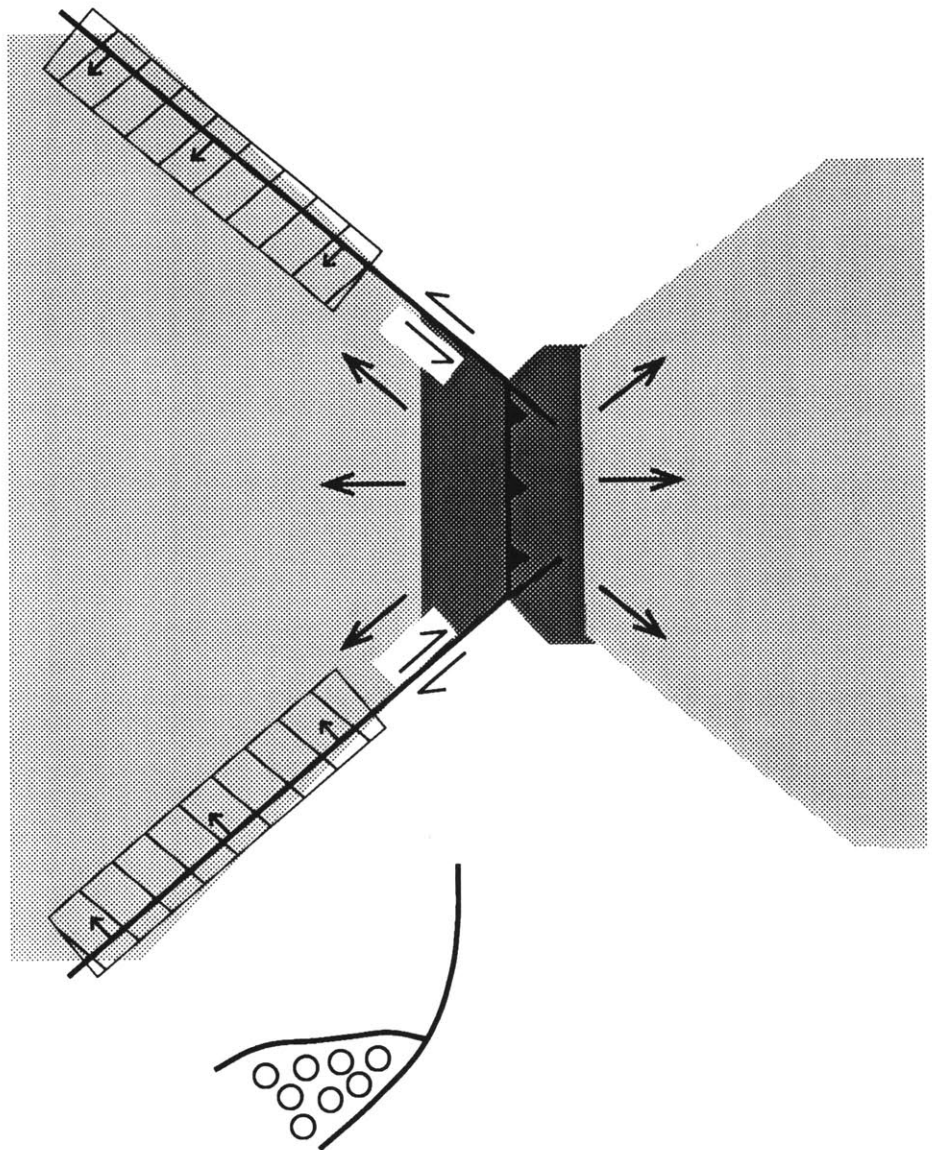
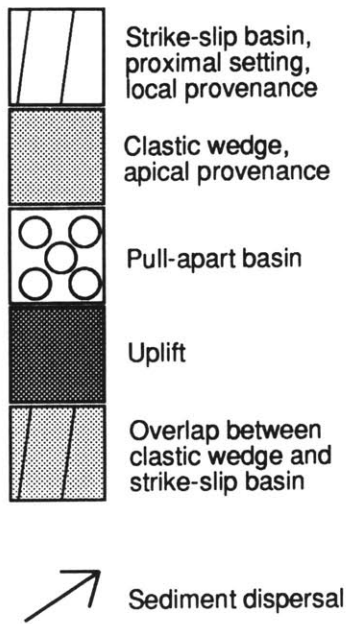


figure 15